"THE SCINTILLATION SPECTROMETER AND ITS APPLICATION IN NUCLEAR TIME-CORRELATION STUDIES"

A THESIS

SUBMITTED TO THE

FACULTY OF GRADUATE STUDIES,

UNIVERSITY OF MANITOBA

IN PARTIAL FULFILMENT

OF THE REQUIREMENTS FOR THE DEGREE OF

DOCTOR OF PHILOSOPHY

by

K. I. ROULSTON

WINNIPEG,

MARCH, 1952.

CONTENTS

ILLUSTRATIONS

PLATES

FIGURES

PREFACE

The work described in this thesis was carried out at the University of Manitoba during the years 1949-52 inclusive.

In presenting it the author wishes to express his sincere thanks to the director of the research - Dr. R. W. Pringle - for his constant interest, encouragement and stimulating discussions, and to Mr. C. Kubin and Mr. G. Trider for their co-operation in the mechanical construction side of the project.

The assistance of the National Research Council of Canada in providing funds for the purchase of much of the equipment is gratefully acknowledged.

SUMMARY

The development of a gamma ray spectrometer based on the scintillation counter as a proportional device is described. The performance of the spectrometer is evaluated by studying the gamma ray scintillation spectra of several radioactive isotopes. Two such spectrometers are then applied to time-correlation studies in nuclear disintegrations using the coincidence technique, with the object of elucidating the decay schemes.

1. INTRODUCTION

Lenard's proposal in 1903 that the atom consisted of a concentrated massive centre, called a "dynamid", round which a cloud of electrons existed was extended by Rutherford in 1911 to explain the phenomenon of radioactivity. Since then physicists have been very interested in finding out more about the structure of the massive centre (or "nucleus" as it came to be called) of the atom.

One of the approaches has been the study of the energy levels which exist in the different nuclei, and this study has been called "nuclear spectroscopy". Intensive work during the last quarter century has resulted in the accumulation of a vast amount of information but a satisfactory theory of the nucleus is still not available. It is the hope of the experimentalist that the continuance of this work may give the theoretician the vital clues to enable him to formulate a sound theory.

In this thesis the application of a new technique to gamma ray spectroscopy is the central theme and the technique is applied not only to the study of gamma ray spectra but also in an effort to correlate the separate gamma ray energies with each other and with certain beta particle (maximum) energies. In this way it is possible to propose decay schemes with considerably more certainty than has hitherto been possible.

2. NUCLEAR SPECTROSCOPIC TECHNIQUES.

One of the essential components of a nuclear spectrometer is a radiation detector. In certain cases the detector itself may provide sufficient information for energy measurements, while, in other cases, additional equipment is necessary.

It is proposed to review the equipment and detectors which have been available for nuclear spectroscopic studies since the discovery of radioactivity. In order to appreciate the advantages and/or disadvantages of the different instruments it must be realised that, as the disintegration of a nuclear species is a random process, the mathematical laws of probability apply to it and, in order to arrive at a conclusive result, a large number of events must be analysed. For this reason it is desirable that a detector should be highly efficient for the particles being considered and that it should be able to deal with large numbers in a short time, in order to make experiments easy to perform.

Becquerel's detector was the photographic plate and this method is used at the present time mainly for cosmic ray studies. Energy measurements can be made by studying track lengths in the emulsion but the process is a tedious one as the time taken to study a track is considerable.

The second detector, much used by Rutherford, was the scintillating screen discovered by Crookes in 1903. The screen was made by causing zinc sulphide powder to adhere to a glass plate. When bombarded by particles or gamma-rays it scintillates,

or flashes, at the points of impact of the particles. An observer was necessary to count the flashes on the screen and hence only low radiation intensities could be used. It is efficient for the detection of alpha and beta particles, but not for gamma radiation. It cannot, by itself, be used for energy measurements and was normally used in the determination of the range of alpha and beta particles, from which the energy could be deduced.

The Wilson Cloud Chamber (1912) provided a very convenient and elegant method of viewing the tracks of ionising particles. In it the particles cause ionisation in a saturated vapour, which thereupon condenses on the ions. The track of the particle thus becomes visible when suitably illuminated. The method lends itself admirably to the photographic recording technique. It is primarily of use in studying the behaviours of individual particles, especially rare events.

The next detector was the Geiger counter (1913), which was an enormous step forward in that it permitted much more rapid counting. An improved version, the Geiger-Muller counter, appeared in 1928 and this has been widely used in experimental work ever since. These counters are efficient for the detection of alpha and beta particles but not for gamma rays. They are not suitable for direct measurements of particle energies and are therefore used in conjunction with other energy measuring

methods. One of these is the absorption technique which has been widely used with very considerable success. Another method is the 180° magnetic focussing spectrometer in which beta particles are focussed at different points depending on their energy. This has provided very accurate beta and gamma energy measurements, as has also a different type of magnetic spectrometer called a lens spectrometer, which uses helical focussing. In these spectrometers the collection efficiency is fairly low; thus, strong sources of 1 to 0.1 millicurie have generally to be used.

Further developments of the Geiger counter are the ionisation chamber and the proportional counter. These suffer from low detection efficiency for gamma rays and very small output pulses, but are capable of energy determinations by the use of a pulse height analyser.

In 1945 Elau and Dreyfus (1) proposed the use of a photomultiplier in conjunction with a scintillating screen as used by Crookes, the radiation intensity being measured by means of a galvanometer. This detector was the forerunner of the scintillation counter, which has overcome the main disadvantages of the other detectors and is now very widely used. High efficiency for the detection of alpha, beta and gamma radiations can be attained by using suitable scintillating crystals. Moreover, as will be discussed in detail below, the scintillation counter acts as a proportional device and

can, therefore, be used for direct energy measurements in conjuntion with suitable pulse-height analysing equipment. Its speed of operation is very high which is an added advantage.

3. THE SCINTILLATION SPECTROMETER.

The first aim of the research programme was the development of a gamma ray spectrometer, based on the scintillation counter.

For a full understanding of the operation of the scintillation counter it is necessary to consider the manner in which radiation and matter interact. There are three well-known ways in which interaction takes place, called respectively the photoelectric effect, the Compton effect and the "pair production" effect.

The photoelectric effect is so called because of its similarity to the photoelectric phenomenon exhibited by a photosensitive surface when light falls on it. This latter photoelectric effect involves the expulsion of loosely bound electrons from the surface by the low-energy photons of visible light. In the case of gamma radiation the photon energies are much higher and there is a much higher probability of tightly bound electrons being expelled. Generally the photoelectrons come from the K and L shells and the process is more likely to occur in atoms of high atomic number, the photoelectric cross-section of a material being roughly proportional to $Z^{4.7} \; E_\gamma^{-3.5}$, where E_γ is the gamma ray energy.

The photoelectron gains energy equal to $E_\gamma - E_K$ or $E_\gamma - E_L$ for K and L shell electrons respectively. The atom becomes excited in this process and the empty shell is quickly filled with the emission of an X-ray(or X-rays in cascade) which,

in turn, gives up its energy to other extra nuclear electrons. Thus, generally speaking, the total gamma ray energy is converted to electronic energy in the matter.

The Compton effect is somewhat different, in that the gamma ray photons collide ~~elastically~~ with loosely bound electrons in the matter and the amount of energy transferred to the electron depends on the angle of collision. The distribution of this energy has a certain form called a "Compton distribution", and the energy not transferred is carried on by a secondary photon. The Compton cross-section is proportional to Z/E_γ (Z) so that it is more pronounced in matter containing elements of high atomic number. The secondary photon, generally having considerably less energy than the primary photon, has a good chance of being subsequently captured photoelectrically, especially if the quantity of material through which it has to pass is appreciable. Thus some gamma rays will give up all their energy to electrons in the matter, while others will give up only a part. Where all the energy is transferred the effect might be called "pseudo-photoelectric" since it is indistinguishable from the true photoelectric effect.

The third type of interaction - pair production - occurs when a high energy photon passes close to the nucleus of a heavy atom. The photon may disappear completely and in its place two charged particles, an electron and a positron

appear having an energy $E_\gamma = 2 m_o c^2$ where $m_o c^2$ is the rest energy of the electron or the positron. $m_o c^2$ corresponds to 0.51 MeV, hence a minimum gamma ray energy of 1.02 MeV is necessary for the pair production process to take place. The pair production cross-section is proportional to $Z^2 f(E_\gamma)$. $f(E_\gamma)$ is zero at $E_\gamma = 1.02$ MeV and increases rapidly as E_γ increases.

The positron resulting from pair production has a limited life and quickly combines with an electron in an "annihilation" process with the production of two photons, each of energy 0.51 MeV. There is, as before, a possibility of one or both of these photons being absorbed in the matter.

Thus it is seen that a photon of energy E_γ, on striking a piece of matter, may lose some or all its energy in three ways:-

(1) an amount E_γ by photoelectric effect.

(2) an amount E_γ by a combination of the Compton and photoelectric effects (pseudo-photoelectric effect) or an amount less than E_γ by the Compton effect alone.

(3) an amount E_γ, $E_\gamma - 0.51$ MeV or $E_\gamma - 1.02$ MeV by pair production, with or without subsequent capture of one or both of the annihilation quanta.

Figure 1, page 9, shows the relative cross-sections of iodine for photoelectric effect, Compton effect and pair

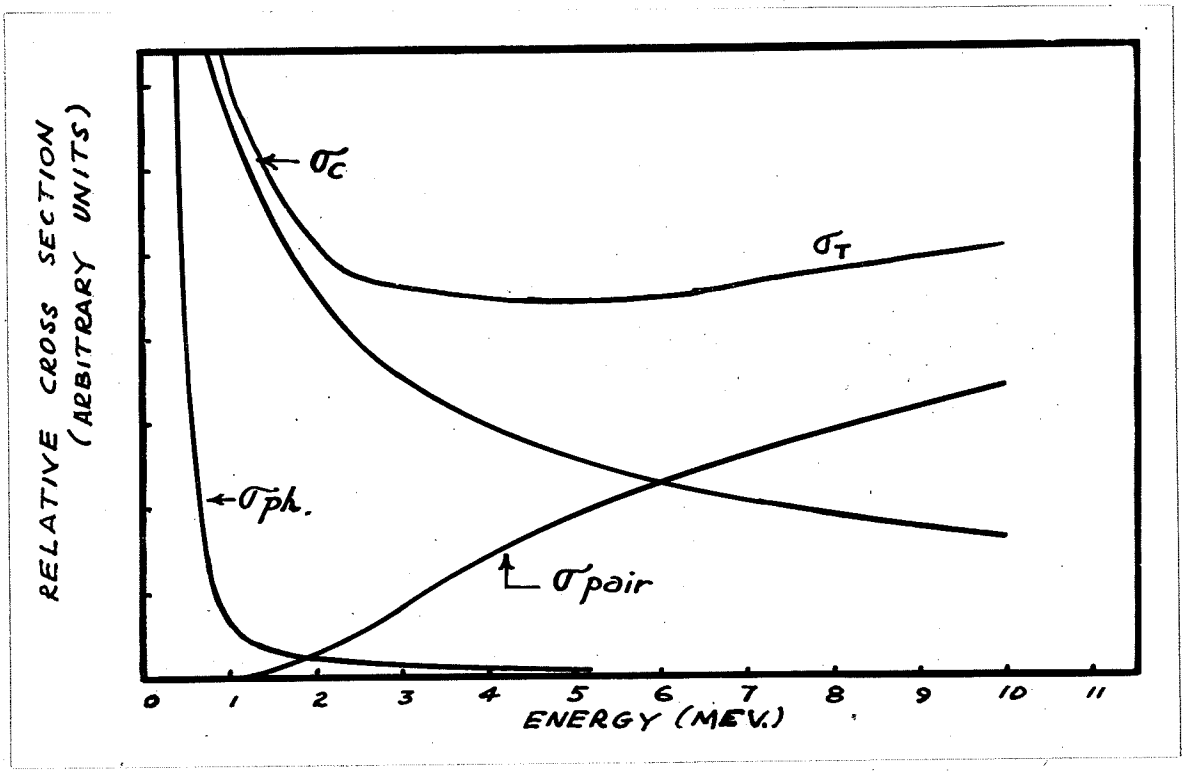

FIGURE 1.

Cross-sections of Iodine

production respectively plotted against the energy of the gamma ray. The total cross-section, which is proportional to the detection efficiency, is the sum of the three individual cross-sections.

If the matter which the gamma ray strikes is a crystal of one of a number of materials, e.g. naphthalene, anthracene, stilbene, sodium iodide (activated with 1% of thallium iodide) etc., the electrons moving in the crystal lattice cause excitation of the atoms and emission of light flashes (or scintillations). The combination of a scintillating crystal (or crystals) and a suitable detector constitutes a scintillation counter.

The amount of light emitted by the crystal is dependent on the energy given to it by the gamma ray and might be expected to be proportional to it, subject to statistical fluctuations. That this is the case over at least a considerable energy range has been verified. This linearity and the matter of statistical fluctuations will be discussed later.

The light flashes should be detectable by a photocell but the amplitudes of the signal pulses are actually so small that they are considerably below the noise level of an amplifier. However, if a photo-multiplier tube is used the signal level can be raised well above the usual noise level and direct observation of the individual pulses becomes possible. (3-8) The output of a photomultiplier is proportional to the light falling on the cathode, for low levels of intensity, subject to statistical fluctuations once again.

By analysing the amplitude distribution of the pulses from the photomultiplier, amplified if necessary, it should be possible to obtain information concerning the relationship between the average pulse height and the energy of the gamma rays causing the pulses.

The complete layout of the equipment as used is shown in Figure 2A. This is in its most general form and for certain purposes some units of equipment are not required, in which case they may be disconnected. A lead castle for enclosing the detector head was available for studies involving weak activities. A discussion of the various units will now be given.

There are two main methods of pulse-height analysis available, using either biassed trigger circuits or electron beam deflection. In the present case the former method was chosen for development first. Both types of analyser require to be preceded by amplifiers as the output available from a photomultiplier is limited to a few volts. For this purpose the Atomic Instrument Co.'s model 204C amplifier was used. It has

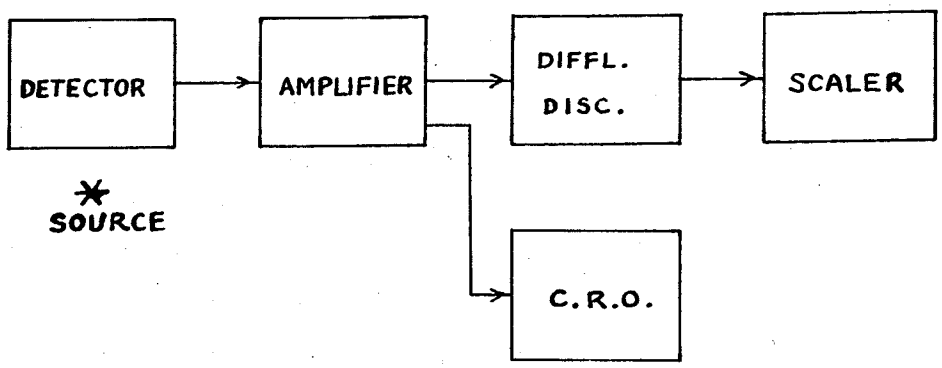

(A) GAMMA RAY SPECTROMETER
BLOCK SCHEMATIC.

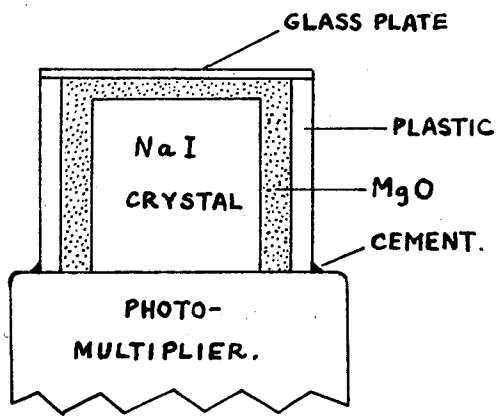

(B) CRYSTAL MOUNT.

FIGURE 2.

an amplification of approximately 5000 times and has facilities for altering the rise time of the amplified pulse and the "clipping" or decay time of the input pulse. It also has an input attenuator with 2 times steps over a range of 32:1, and is able to accept either positive or negative input pulses. The output pulses are positive and may be up to 80 volts in amplitude. The overload characteristics of the amplifier are reasonably good. Pulses of 10 to 20 millivolts from the photomultiplier will provide reasonably sized output pulses for analysis. In practice it was found that pulses of about 1 or 2 volts could be obtained from a photomultiplier without noticeable distortion and for this reason further amplifiers of simple design and smaller amplification (about 60 times) were constructed. The circuit for these amplifiers is shown in Figure 3 and is substantially the same as the latter portion of the model 204C amplifier. Because of the low impedance input attenuator (1600 ohms), it was necessary to feed the pulses from the photomultiplier through a cathode follower in order to avoid loss of amplitude. This cathode follower was built into the scintillation counter assembly and the circuit diagram for the whole is shown in Figure 4.

A standard stabilised power supply was used throughout to supply power to cathode followers, amplifiers and other units. The design shown in Figure 5 was used and proved to be adequate. Where extra high stability was required the power

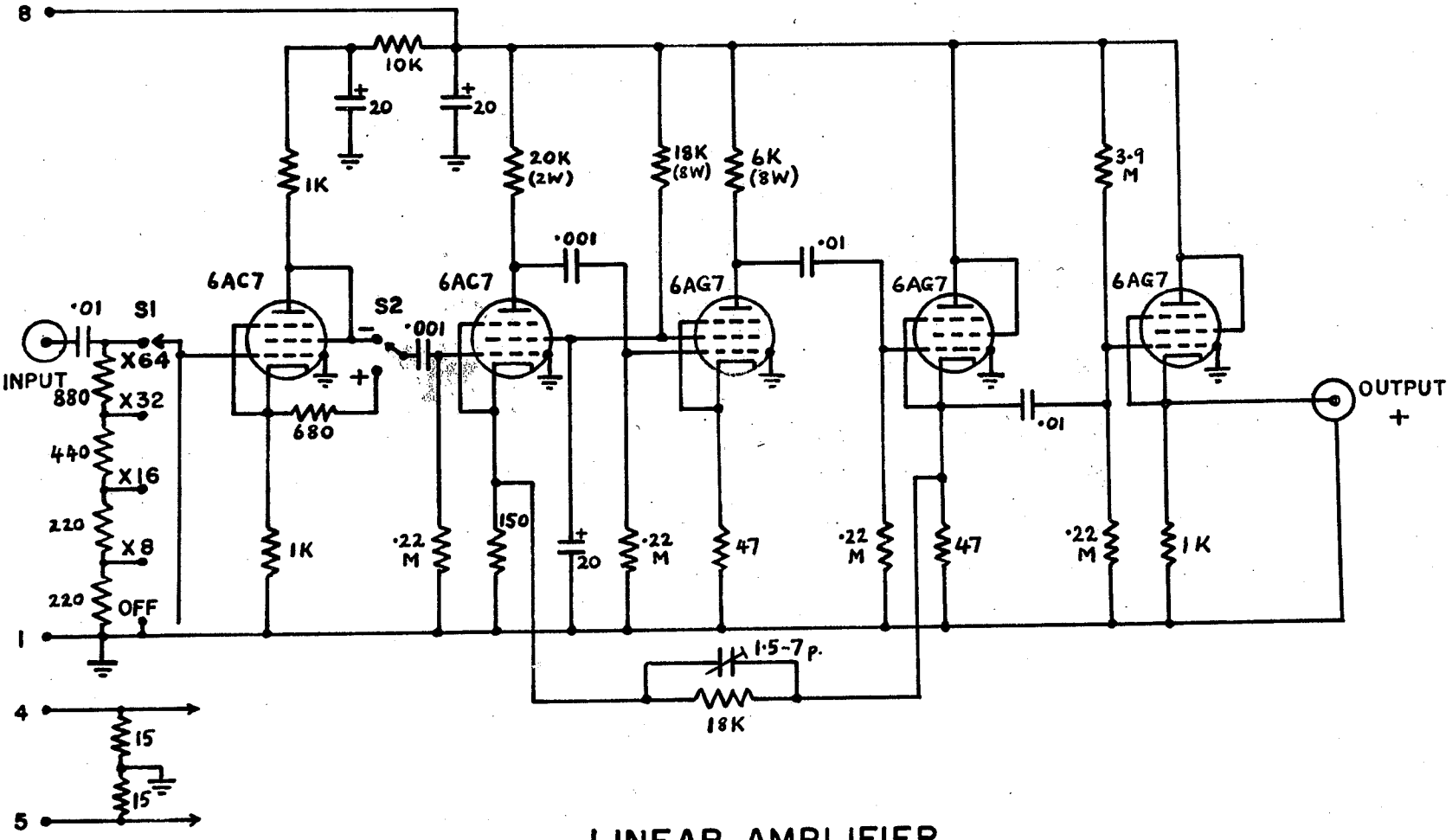

LINEAR AMPLIFIER.

FIGURE 3.

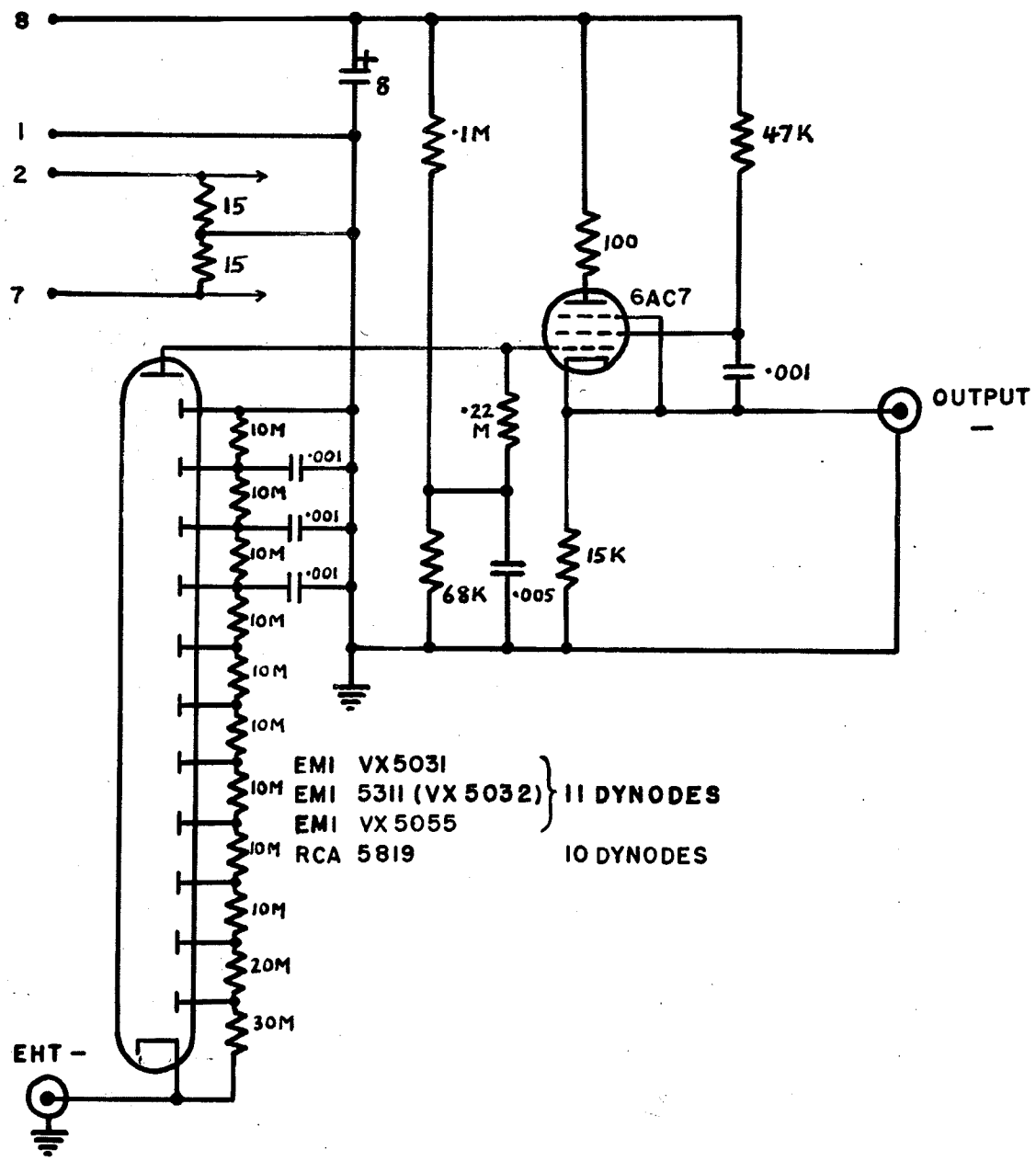

PHOTOMULTIPLIER AND
CATHODE FOLLOWER CIRCUITS.

FIGURE 4.

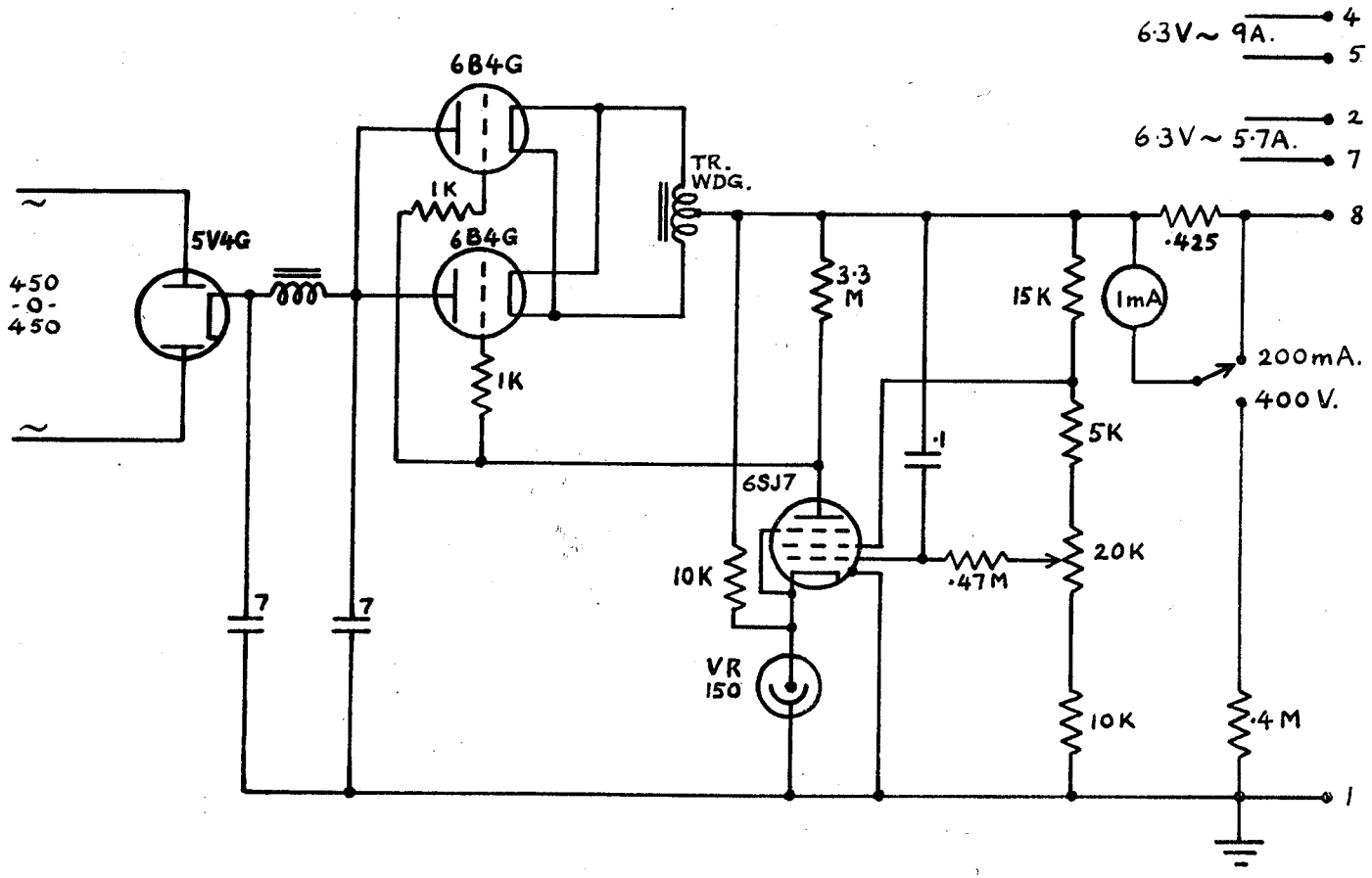

STABILIZED POWER SUPPLY.

FIGURE 5.

unit was run off a stabilising transformer. A model 1007 high voltage stabilised power supply (A.E.R.E.) was used to supply all photomultipliers with appropriate voltages. It might be mentioned that a 1% change in the voltage applied to a photomultiplier of 10 stages causes a change of about 7% in the gain of the photomultiplier. If a 0.5% stability in the complete equipment is being aimed at, the photomultiplier voltage should be stable to about 0.01%.

Pulse height analysis employing trigger circuits may be performed in a variety of ways. The simplest method is to obtain what is called an "integral" bias curve in which all pulses greater than a certain amplitude are recorded and all pulses less than this amplitude are rejected. This amplitude (of discrimination) is equal to the bias which is applied to the trigger circuit beyond the bias at which the circuit will run freely (or trigger with zero amplitude of signal). Such a bias curve is of limited value. It will show, to a certain extent, if a scintillation counter is acting in a proportional manner and a pulse height distribution curve (or differential bias curve) can be constructed from it, by plotting the difference in counting rates between successive points on the integral curve. However, since the events being counted are random in nature it can be shown that the uncertainty in the differential curve readings will be considerable when the readings for points on the integral curve are taken over non-con-

current time intervals (9).

Suppose, for example, that, for a point on the integral curve, N_1 counts are obtained in a time t and that N_2 counts are obtained for an adjacent point in a period of the same duration, t, but not concurrent with the count on the first point. The standard deviations, assuming a Gaussian distribution, are respectively $(N_1)^{\frac{1}{2}}$ and $(N_2)^{\frac{1}{2}}$. The difference reading is N_1-N_2 but the standard deviation is $(N_1+N_2)^{\frac{1}{2}}$. Thus, if N_1 and N_2 are nearly equal, the percentage error possible in the difference is very large unless N_1 and N_2 are themselves very large. On the other hand, if the two counts are made concurrently so that all the counts N_2 arise from events which give counts in N_1 as well, the standard deviation is $(N_1-N_2)^{\frac{1}{2}}$. Thus it is seen that, as far as the differential curve is concerned, concurrent counting on adjacent points is highly desirable and results in a great saving of time over the method of non-concurrent counting, when a certain accuracy is required.

N_1 and N_2 can be determined simply by a pair of electronic trigger circuits biassed to different levels, each feeding into a scaler. But the difference N_1-N_2, in which we are really interested, may be obtained by using a subtraction or anti-coincidence circuit following the two trigger circuits, with a saving of one scaler as well.

It was envisaged that the scintillation counter would be used in coincidence experiments eventually, and for this reason it was considered desirable to make the pulse height analyser as simple as possible to avoid the introduction of time delays which are inevitable in complicated circuitry. The circuit arrangement finally adopted is shown in Figures 6 and 7, which show respectively the trigger circuits and the anti-coincidence circuit, and is substantially the same as a simple pulse height analyser previously described by the author (10).

Each trigger circuit consists of a modified Schmitt trigger circuit (11-14) and operates as follows:- a positive pulse is applied to the first tube which is biassed beyond the cut-off point by a predetermined amount. If the pulse is larger than the bias, it causes the tube to conduct, and the negative pulse developed at the anode is applied to the grid of the second tube. This causes the cathode potential to fall and thereby increases the current flowing in the first tube. The process is cumulative and the second tube is quickly cut off. The positive pulse appearing at its anode is of constant amplitude, irrespective of the amplitude of the input pulse provided it is large enough to trigger the circuit. The positive pulse is fed into an inductance shunted by a crystal diode, which gives it the shape of half a sine wave whose duration is roughly 0.5 microseconds.

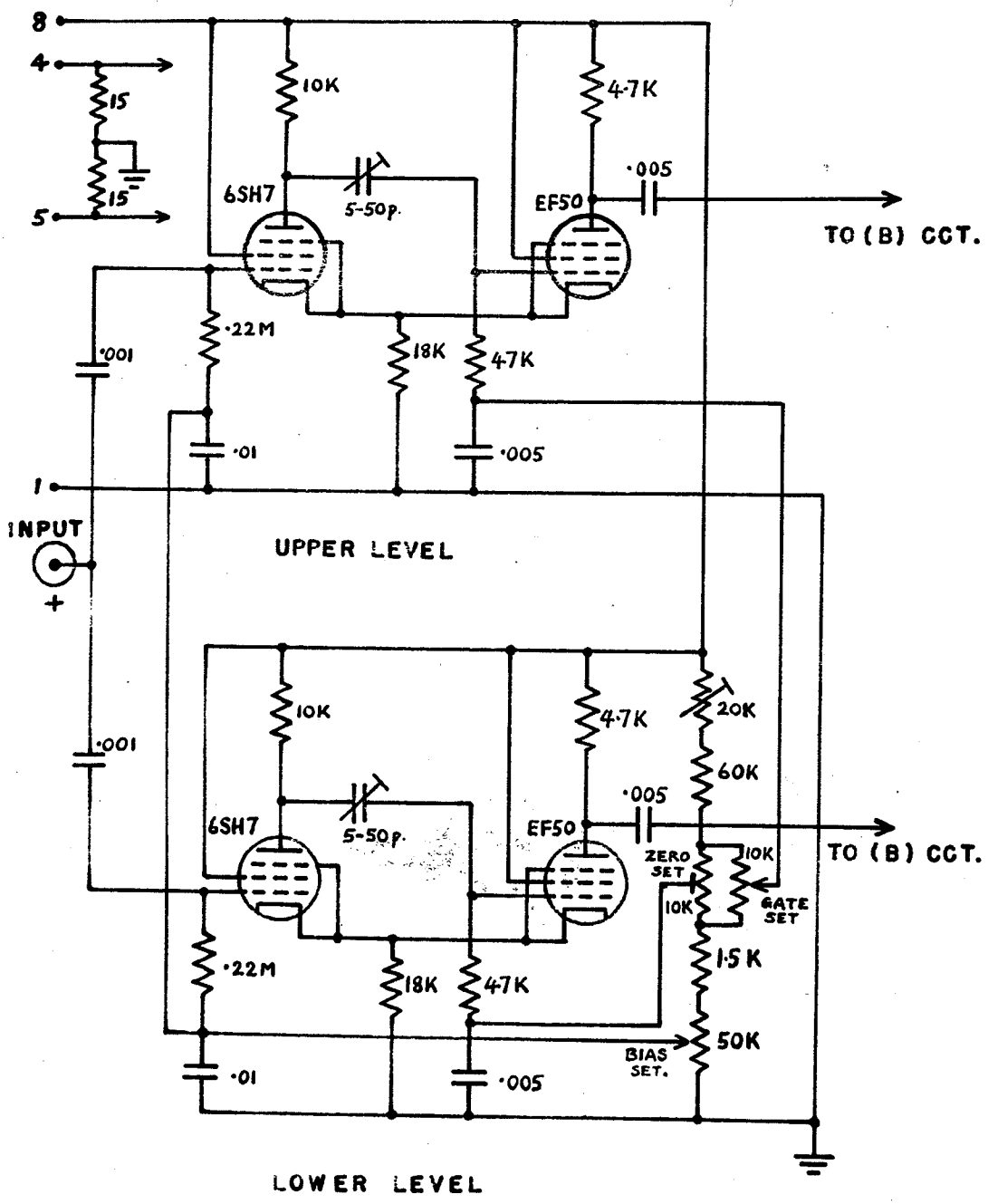

DIFFERENTIAL PULSE-HEIGHT ANALYZER
(A) DISCRIMINATOR CIRCUITS.

FIGURE 6.

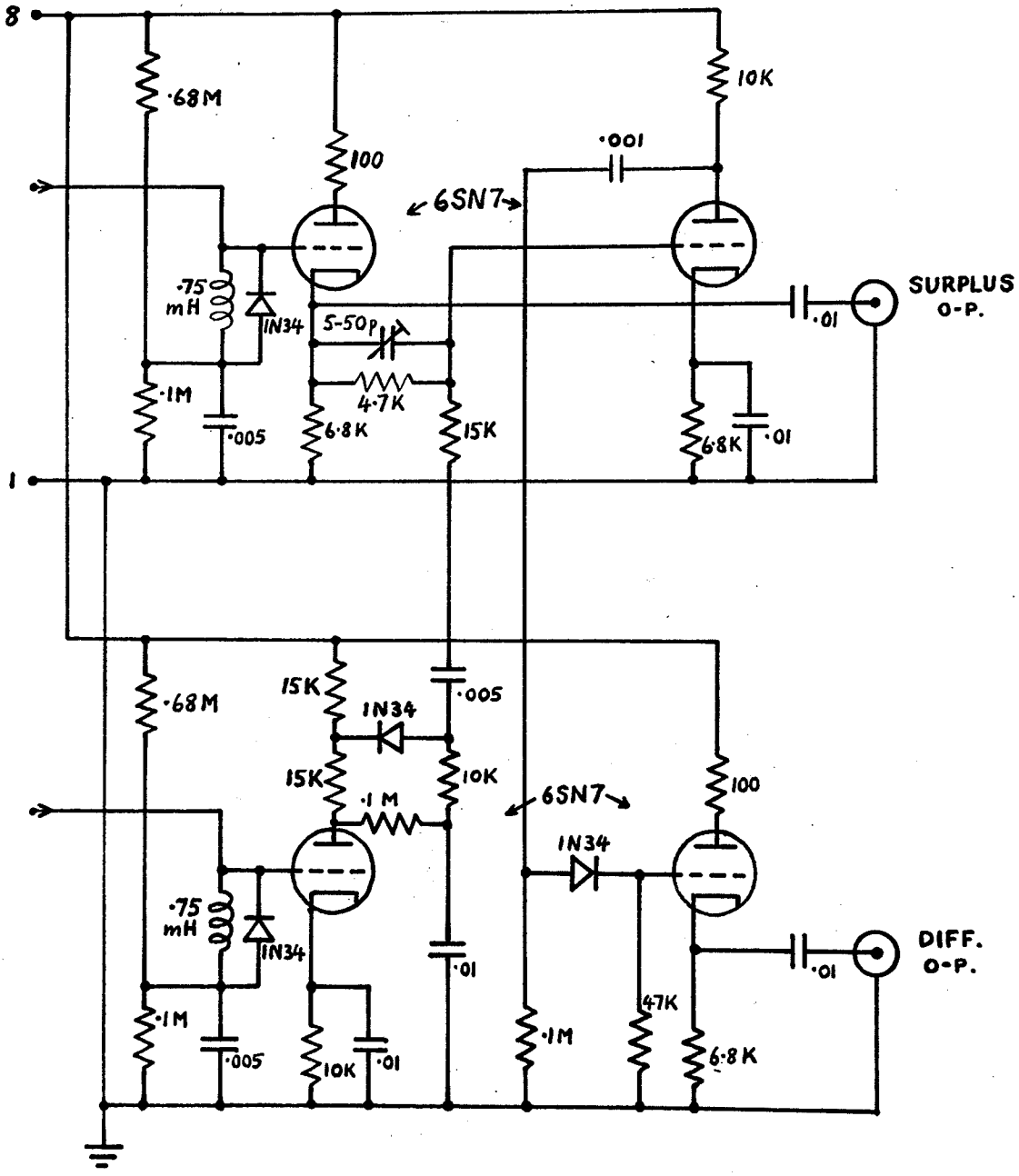

DIFFERENTIAL PULSE-HEIGHT ANALYZER
(B) ANTI-COINCIDENCE CIRCUIT.

FIGURE 7.

The Schmitt circuit employs direct coupling between the anode of the first tube and the grid of the second tube. Consequently the bias voltages for the two tubes are obtained from different resistance chains and this may lead to drift in the equipment. In the modified circuit used here both voltages are obtained from one resistance chain, and drifts in voltage affect both tubes approximately equally.

For the anti-coincidence circuit the pulse from the lower level trigger circuit is inverted and added to the output pulse, if any, from the upper level trigger circuit through a resistance chain. If both trigger circuits "fire" the two pulses cancel out, while if only the lower fires a resultant pulse is obtained. This is amplified and fed to a scaler or to coincidence equipment depending on the requirements of the experiment to be performed. Owing to the fact that a pulse entering the analyser has a finite rise time (0.2 microseconds or thereabouts) there is generally a small time interval between the firing of the two trigger circuits, when a sufficiently large pulse is received. To ensure adequate cancellation in the anti-coincidence circuit only the peak of the pulse from the lower level trigger circuit is used, by employing a biassed crystal diode in the anode circuit of the tube used to invert it. Cancellation of the pulses is not always complete but by choosing a suitable discrimination level on the following equipment it is possible to exclude the unwanted pulses. A graph giving the integral amplitude distribution of the pulses

from the anti-coincidence circuit is shown in Figure 8, and also a graph showing the counting rate of the output pulses plotted against the difference in bias level between the two trigger circuits. This shows that the fringes of the voltage amplitude interval or "gate" are reasonably sharp.

For the purpose of testing the pulse height analyser and the linear amplifiers, a small pulse generator was constructed using a thyratron as a relaxation oscillator. The circuit which is shown in Figure 9 is of fairly standard design. Output pulses of up to 10 volts (either positive or negative) are obtainable. The pulse duration is about 2 microseconds and the repetition frequency can be altered between 40 and 1000 pulses per second approximately.

For straightforward gamma ray spectroscopy, the differential pulse height analyser is followed by a scaler and two models were available; viz.- the Atomic Instrument Co.'s model 105 (scale of 1000) and the A.E.R.E. model 1009 (scale of 100).

A four-channel pulse height analyser model 1074 (A.E.R.E.) became available in the later stages of the programme and was of great value as a time-saver in investigations requiring long counting times.

A Tektronix model 511 A D cathode ray oscilloscope was also obtained and this was used not only for test purposes, but also for displaying the pulses from the linear amplifier, each pulse triggering the time base. By photographing the

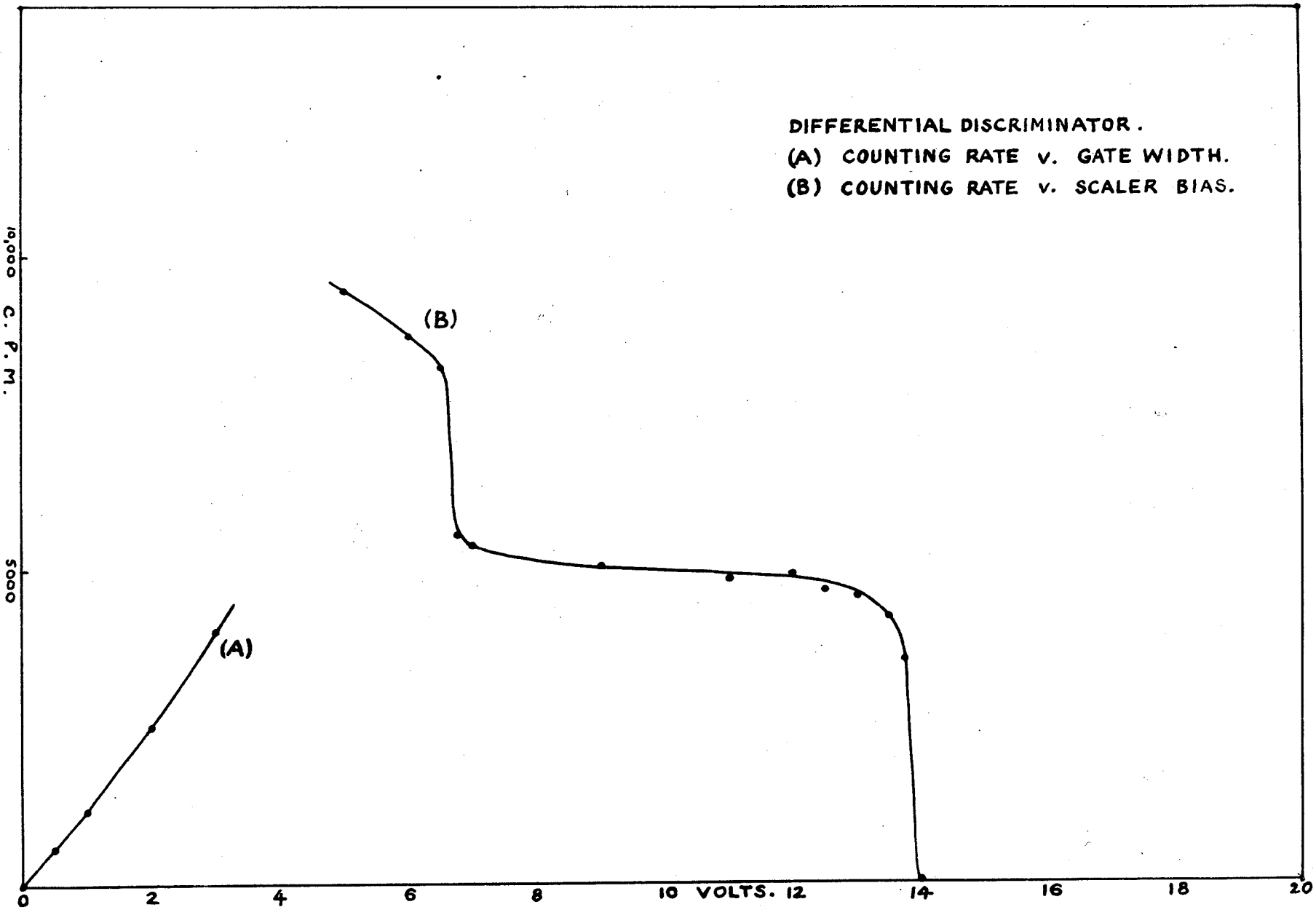
DIFFERENTIAL DISCRIMINATOR.
(A) COUNTING RATE v. GATE WIDTH.
(B) COUNTING RATE v. SCALER BIAS.
10,000
C. P. M.
5000
(A)
(B)
0
2
4
6
8
10 VOLTS. 12
14
16
18
20

FIGURE 8.

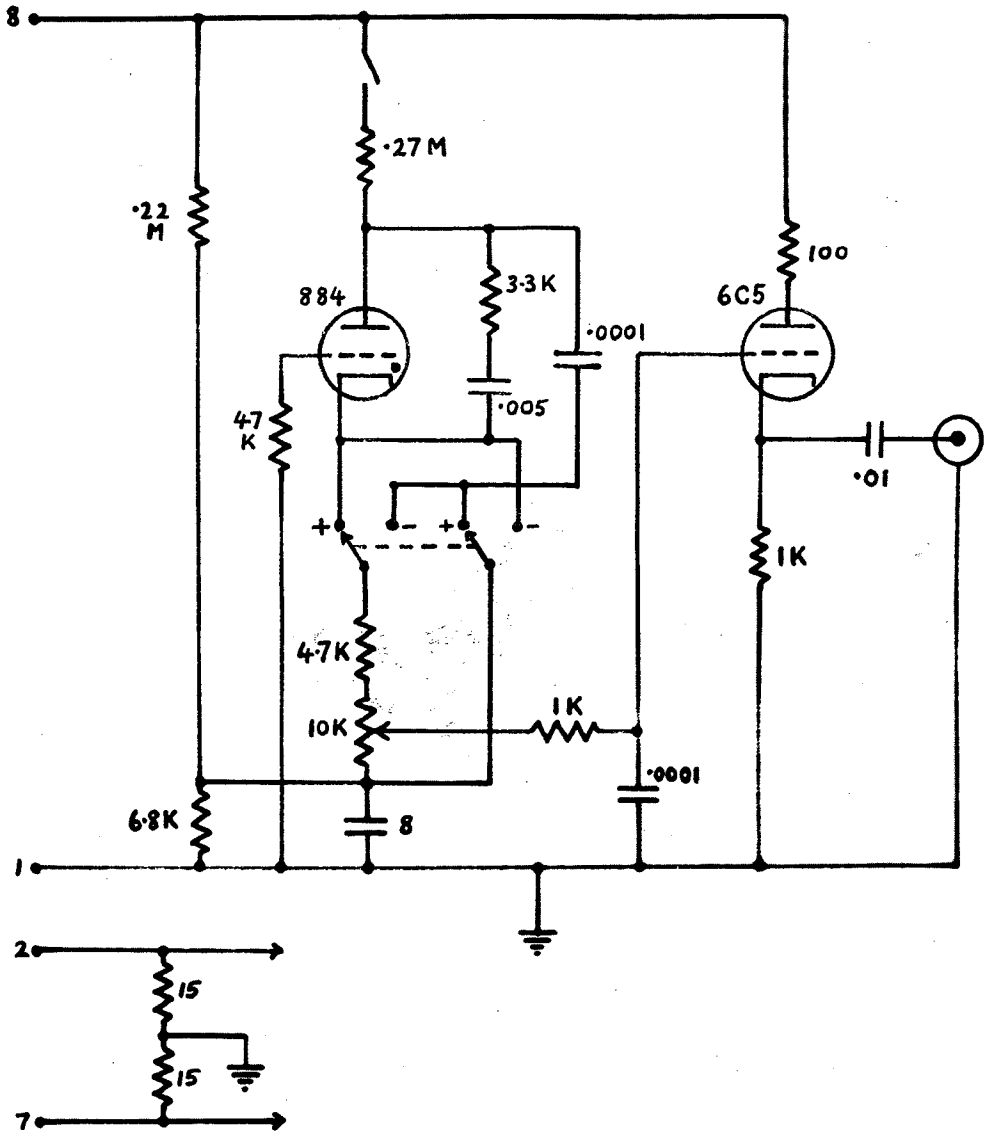

PULSE GENERATOR.
FIGURE 9.

screen for a suitable time, photographs showing the complete pulse height distribution were obtained.

A recent method of display is to feed the pulses as flat-topped waves (of amplitude equal to the pulse height) to the Y plates of the cathode ray tube and modulate the intensity of the electron beam by applying an exponentially varying voltage to the cathode of the tube, causing the trace to become dim as it moves to the right. By this means an exponential intensity scale on the cathode ray tube screen is obtained, and a whole spectrum can be photographed at once, irrespective of large intensity variations between the different lines.

Of all the possible scintillating crystals, it was known that sodium iodide activated with 1% of thallium iodide produced most light energy per KeV of gamma ray energy. From the statistical treatment below it will become apparent that the efficiency of conversion of gamma ray energy to light energy is very important. But more important still is the fact that sodium iodide is one of the few scintillating crystals which has in its lattice an element of relatively high atomic weight. This is highly desirable in order to enhance the photoelectric effect relative to the Compton effect. Sodium iodide (activated) crystals of high optical grade were available at the time. For these reasons sodium iodide was chosen as the scintillator for the initial experiments and it

proved so successful that it has been used ever since.

The R.C.A. 1P21 photomultiplier was first used in experiments but it has an internal cathode which presented a difficulty in getting light from the crystal to the cathode. This was later replaced by the R.C.A. 5819 photomultiplier, which has a transmission type cathode deposited on the glass envelope at one end of the tube. This proved to be a considerable advance. E.M.I. also produced a photomultiplier (type 5311) with a similar type of cathode, and it was found to be considerably better than the average R.C.A. 5819. This tube (5311) has been used for all the finer detailed work where maximum resolution is desirable.

Early tests (April 1949) with an integral "discriminator" indicated that the scintillation counter did behave as a proportional device and gave reason to believe that it could be developed into a useful gamma ray spectrometer. Compton distribution curves were obtainable but photoelectron lines did not tend to be clearly resolved. However, this was not surprising as very long counting times were necessary to get reasonable statistical accuracy, and, in addition, the source used in early tests was cobalt 60 for whose gamma rays iodine (the chief component of the crystal) does not have a large photoelectric cross-section. Later (August 1949), using a differential pulse height analyser and iodine 131, whose main gamma rays are of much lower energy, photoelectric peaks on the distribution curve were obtained. This enabled quantitative

tests to be made on crystals, crystal mountings (reflectors, etc.) and geometry.

Extensive tests were carried out on crystal mountings. Identical electronic conditions were used for all the tests and the 364 KeV gamma ray from iodine 131 was used for purposes of comparison of the different methods of mounting. The mean amplitude of the pulses arising from this gamma ray was used to determine the relative light collecting efficiency of each method. Table 1, below, indicates the relative pulse heights obtained.

Table 1.

	Method of mounting crystal	Pulse height
(1)	Polished crystal surfaces, aluminum foil reflector, silicone grease optical bond. (crystal size 1" dia. x 1" long)	9.9
(2)	Roughened crystal surfaces, MgO reflector, crystal enclosed in plastic case with plastic window between crystal and P-M.	9.8
(3)	As (2) except polished surface next P-M.	10.8
(4)	As (3) omitting plastic window between crystal and P-M.	14.4
(5)	As (4) with all crystal surfaces highly polished.	20.2
(6)	As (5) with small crystal ½" x 1" x 1".	29.7

The method of crystal mounting adopted as a result of the above tests is as follows. In order to prevent moisture

getting at the crystal, which is very hygroscopic, a plastic tube is cemented to the cathode of the photomultiplier (see Figure 23).

The crystal is polished on all sides and a layer of silicone grease is smeared over the crystal on the face to be mounted on the photomultiplier. The crystal is then firmly pressed on to the photomultiplier and surrounded by magnesium oxide powder. A greased glass plate is then placed over the end of the plastic tube to exclude further air from the crystal chamber. This procedure should normally be carried out in a "dry box". The effectiveness of a particular type of mounting was judged by the average amplitude of pulses obtained for the 364 KeV iodine 131 gamma ray.

Small clear crystals are found to give the best response, particularly for low energy gamma rays. However, at higher energies, owing to the photoelectric and Compton cross-sections falling off, only small photoelectric peaks at best are available. If larger crystals are used secondary Compton photons are more easily captured and the pseudo-photoelectric effect is appreciable. As an example, the curve for cobalt 60 shows the photoelectric peaks for the 1.17 and 1.33 MeV gamma rays on the Compton edge, using a cylindrical crystal 1 inch in diameter and 1 inch long. If a small crystal had been used these would not have been so definite. In a similar way the large crystal enables some of the annihilation quanta to be captured following the pair production process, and results

in peaks at the full gamma ray energy and also at 0.51 MeV lower down. The normal pair production peak occurs at 1.02 MeV below the gamma ray energy. The thorium spectrum shown in Figure 14 is a good example of this.

It has been shown (15) that the pulse height distribution on a photoelectric or pair production peak has the shape of the Gaussian distribution curve, so that statistical analysis based on this distribution is possible.

To review, the scintillation counter detection process consists of the conversion of the gamma ray energy to photons (of low energy) in the crystal, and the photons give rise to photoelectrons at the photomultiplier cathode. The photomultiplier then increases the electron stream by many stages of multiplication using the process of secondary emission. In the gamma ray to low energy photon conversion the efficiency is not high, (about 5% for sodium iodide). Also the efficiency of the photomultiplier cathode in emitting electrons for photons striking or passing through it is not high (2-5%) and, further, many photons originating in the crystal do not even reach the cathode, being scattered at various surfaces in their path. The result is that the greatest proportionate statistical variations occur in the photoelectrons emitted by the cathode of the photomultiplier, and this variation is kept small by ensuring that -

(1) an efficient scintillator is used, (e.g. sodium iodide, thallium activated),

(2) as many as possible of the photons created in the crystal reach the cathode of the photomultiplier, by using a suitable reflector round the crystal and a good optical bond between the crystal and the photomultiplier, and

(3) the photoelectrons from the cathode are collected efficiently by the first dynode by using a high voltage on the first stage.

If a number, N, of photoelectrons is released from the photomultiplier cathode on the average for a gamma ray of a certain energy causing the crystal to scintillate, there will be statistical fluctuations from this value and the standard deviation will be $(N)^{\frac{1}{2}}$. These fluctuations will give rise to a Gaussian distribution in the photoelectric or pair-production peak for this gamma ray, and the width of this curve at half height will be $2\ (2\ln 2)^{\frac{1}{2}}\ S$ where S is the standard deviation. There will also be fluctuations in the multiplier multiplication and these will cause the half-width to be increased by $(r/r-1)^{\frac{1}{2}}$ where r is the stage multiplication in the multiplier. (16, 17)

The fractional resolution (R) on a line is defined as the width at half height divided by the mean value of the centre of the peak.

Thus $$R = \frac{2(2\ln 2)^{\frac{1}{2}}\ N^{\frac{1}{2}}\ (r/r-1)^{\frac{1}{2}}}{N}$$

or $$R^2 = \frac{4 \times 2 \ln 2 \times 4/3}{N}$$

if we take r = 4 which is a representative value for the photomultipliers in question.

Assuming for the moment that the average number of electrons is proportional to the gamma ray energy, it follows that R^2 should be proportional to $1/E$. Resolutions have been measured over a considerable energy range and the results plotted on a logarithmic scale are shown in Figure 10. A straight line is obtained up to energies of approximately 1 MeV and above this energy the resolution seems to be worse than is to be expected. The slope of the line is $-\frac{1}{2}$ in agreement with theory.

If we take the resolution and energy for a point on the linear portion of the curve and substitute in the above equation for R^2 we find that the number of electrons per KeV comes out to be very close to 2. This agrees quite well with the results of other workers.

The loss of resolution in the spectrometer at higher energies has been noticed by Scherer and Bernstein (19) who report a departure from the linear relationship between R^2 and E^{-1} at an energy of approximately 80 KeV. This is very much lower than in the present investigations and can probably be attributed in part to the use of the R.C.A. 5819 photomultiplier by these workers, whereas the writer has used only an E.M.I. 5311 tube. The uniformity of the cathode in the latter is very much better than in the former, and this is known to affect resolution. In addition, crystal size and geometry are bound to affect the resolution. For example, high energy electrons can escape through

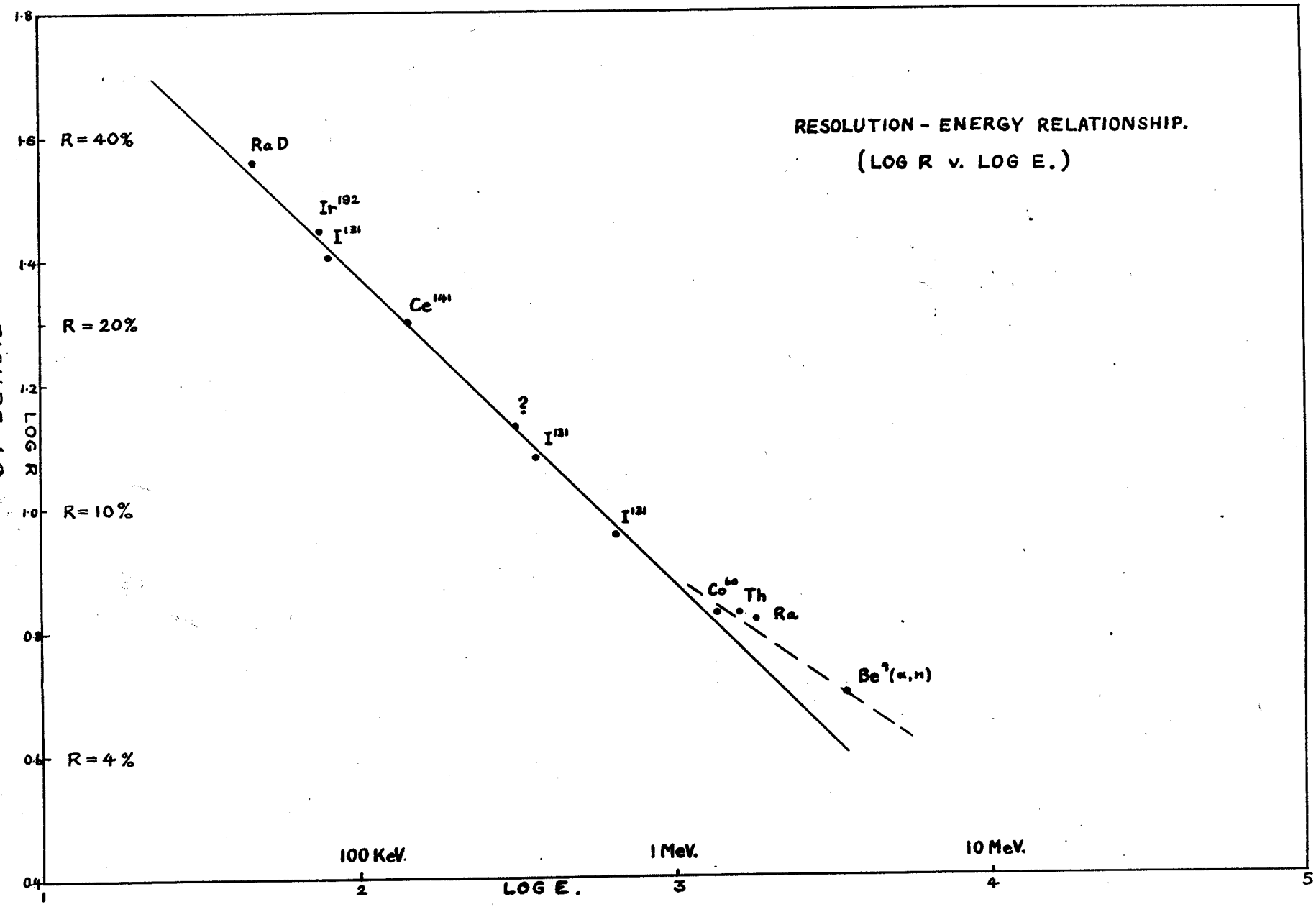
RESOLUTION - ENERGY RELATIONSHIP.
(LOG R v. LOG E.)
R = 40%
R = 20%
R = 10%
R = 4%
LOG R
LOG E.
1.8
1.6
1.4
1.2
1.0
0.8
0.6
0.4
1
2
3
4
5
100 KeV.
1 MeV.
10 MeV.
Ra D
Ir192
I131
Ce141
?
I131
I131
Co60
Th
Ra
Be9(α,n)

FIGURE 10.

the sides of a small crystal more easily, on the average, than from the large crystals, and this gives rise to a preponderance of small pulses thus distorting the normal distribution. In the present work a 1-inch diameter cylinder approximately 1 inch long was used.

Although the resolution of the instrument does not improve as much as it should at high energies there is, nevertheless, proportionality between the mean pulse height and the energy of the gamma ray being detected, over a considerably greater range. Iodine 131 has a good range of gamma rays and provides a means of checking on linearity over the range from 80 KeV to 638 KeV. The 364 KeV line has been used for calibration purposes in conjunction with the attenuator on the amplifier, and no departures from linearity beyond the accuracy of the equipment have been detected, either in measurements of X-ray energies or of high energy gamma rays up to almost 3.5 MeV. In the study of neutron capture gamma rays higher energies are obtained and if, in the example given in this thesis (for aluminum), the end-point value of 7.72 MeV as given by Kinsey, Bartholomew and Walker (18) is taken as correct, there is every reason to believe that the scintillation spectrometer is linear to this energy.

The use of the attenuator on the amplifier as a means of altering the effective gamma ray energy by a factor of E^n is very convenient for calibration purposes, and permits the

use of one source (e.g. iodine 131) to cover the range of energies from 10 KeV to 10 MeV. The attenuator might conceivably not be linear for pulses of duration 1 microsecond, but the maximum output impedance of the attenuator and cathode follower is about 400 ohms, and with stray capacitances of approximately 10 micromicrofarads a delay of only 0.004 microseconds is introduced at worst. The greatest error which might be expected with the present equipment combination is less than 1%.

4. INVESTIGATIONS WITH THE GAMMA RAY SPECTROMETER.

4.1. Geological applications.

To gain experience with scintillation counters, pending the acquisition and assembly of equipment, a portable (battery operated) scintillation counter was constructed and put into use in April 1949. This consisted of a 1 P 21 photomultiplier, a sodium iodide (thallium activated) crystal, a simple amplifier and a trigger circuit with variable bias. The trigger circuit was also used as a counting rate meter by passing the current of one of the tubes through a microammeter shunted by a suitable condenser to give an integrating time of about 10 seconds.

The instrument proved to be of extreme value, not only for monitoring purposes but also for geological application in the discovering of radioactive ore bodies. Moreover, the variable bias feature on the trigger circuit was used to plot integral pulse height distribution curves, and enabled uranium ores to be distinguished from thorium ores to a certain degree. Survey work was carried out in June and July 1949 over territory in the Lake Athabaska and Black Lake regions of N. Saskatchewan where considerable deposits of uranium ore had already been reported. (20-22)

A new technique for displaying radioactive intensities over an area was developed. This was to join up points of equal radiation intensity by lines for which the term "isorad" was coined. A much clearer picture of the distribution of active ore bodies was obtainable. This method was possible because of

the increased stability and much higher statistical accuracy obtainable with the instrument than was hitherto available with the Geiger type of survey instrument. Some new ore bodies were found, as well as extensions to known bodies and, in many cases, the geological structure of a region was clarified by an examination of the radiation maps.

A counting rate of about 10 counts per second was obtained for the background over a non-active area, and with an integrating time of 10 seconds the probable error is about ±7%. A sensitivity of 10^{-10} roentgens per second was thus achieved, and it was possible to detect economic ore bodies at distances up to several hundred feet. It is emphasized, moreover, that because of the instrument's high gamma ray detection efficiency the cosmic ray contribution to the total counting rate was negligible.

Tests in flight indicated that a detector of this type was feasible for aerial prospecting. With the consequent enormous increase in the speed of covering territory, this assumes great importance in a country such as Canada with its vast areas of potential radioactive ore-bearing rocks.

Subsequently, a much more sensitive airborne instrument was constructed and has been in constant use in the search for oil. Oil fields appear to cast a radioactive "shadow" in that radiation intensities over them appear to be low. Such decreases are detectable and may, in conjunction with other geological information, be interpreted to indicate the existence of oil in a region.

This work, however, is rather outside the scope of the present thesis, and so will not be further discussed.

4.2. The gamma rays of cobalt 60.

Cobalt 60 undergoes beta decay and the resultant nickel 60 nucleus emits two gamma rays in cascade (23). The energies of these gamma rays have been measured very accurately (24), and the values given are 1171.5 ±1.0 KeV and 1331.6 ±1.0 KeV respectively.

Because of this simple decay scheme, the accurate measurements on the gamma ray energies and the fact that the half-life is 5.2 years (25) have made cobalt 60 a very convenient gamma ray reference standard.

Early measurements on cobalt 60 with the scintillation spectrometer in its development stage showed clearly a Compton distribution with a faint trace of inflexions on the Compton edge. These were attributed to the photoelectric effect of the two gamma rays.(26) At the same time a comparison of this curve with that obtained for iodine 131, indicated linearity between the gamma ray energy and the pulse height arising from the gamma ray.

Many small points have contributed to improving the performance of the spectrometer; e.g. improvements in the electronic equipment, the employment of more efficient photocells, the choice of more suitable crystal shapes and improved methods of getting light out of the crystal. The result is that the cobalt 60 curve which is now obtained with the spectrometer is very different from that of 2½ years ago. (See Figure 11). The pseudo-photoelectron lines stand out clearly

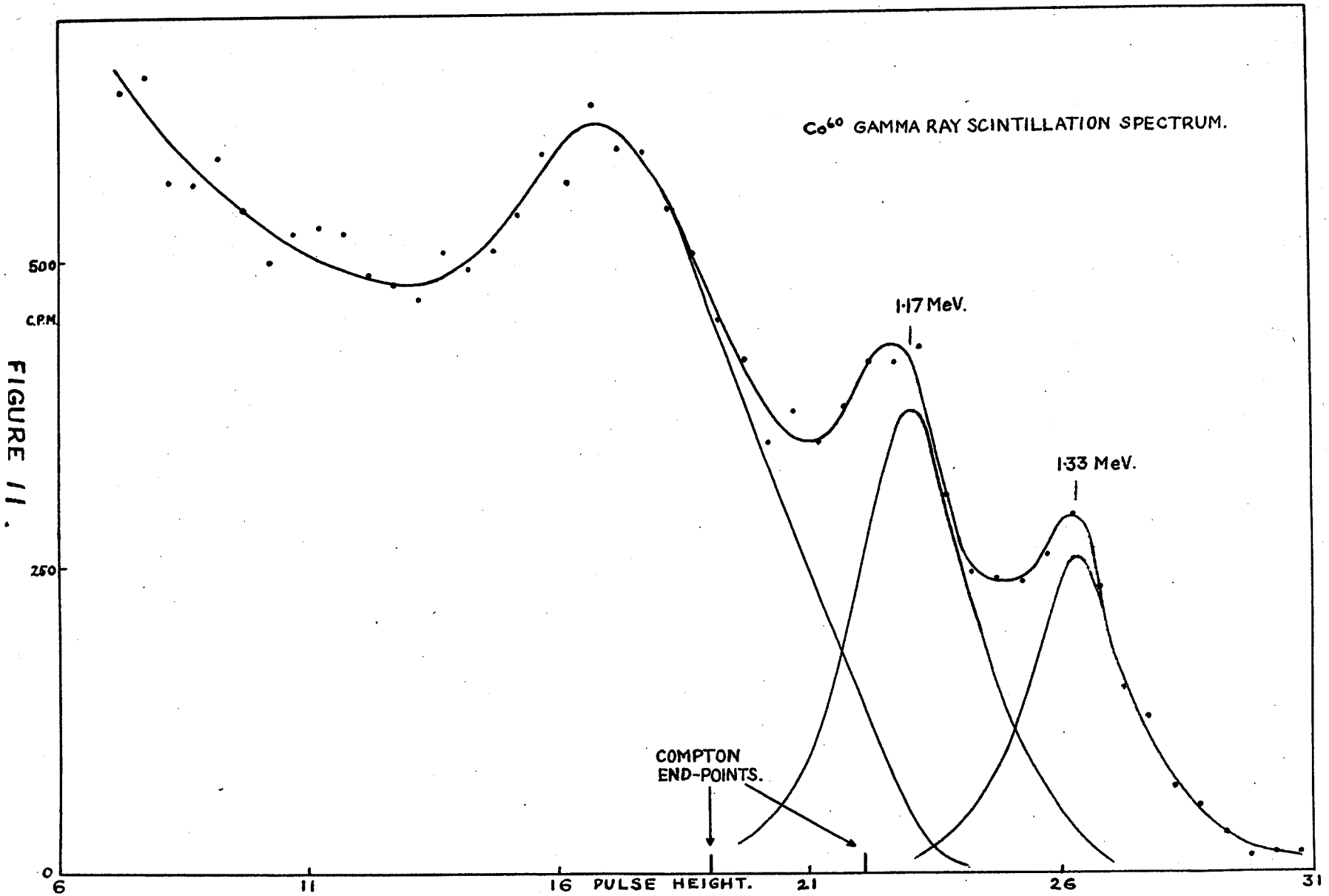
Co60 GAMMA RAY SCINTILLATION SPECTRUM.
500
C.P.M.
250
0
1·17 MeV.
1·33 MeV.
COMPTON
END-POINTS.
6
11
16
PULSE HEIGHT.
21
26
31

FIGURE 11.

and the gamma ray energy values are in very good agreement with the values given by Lind et al (24). At one stage the Compton peaks for the two gamma rays appeared to be resolved (17), but with the enhanced photoelectric effect the Compton peaks appear now to be less well separated.

Plate 1 is a photograph of the pulse height distribution on a cathode ray oscilloscope. The peak on the Compton distribution is clearly visible with the two photoelectron lines above it.

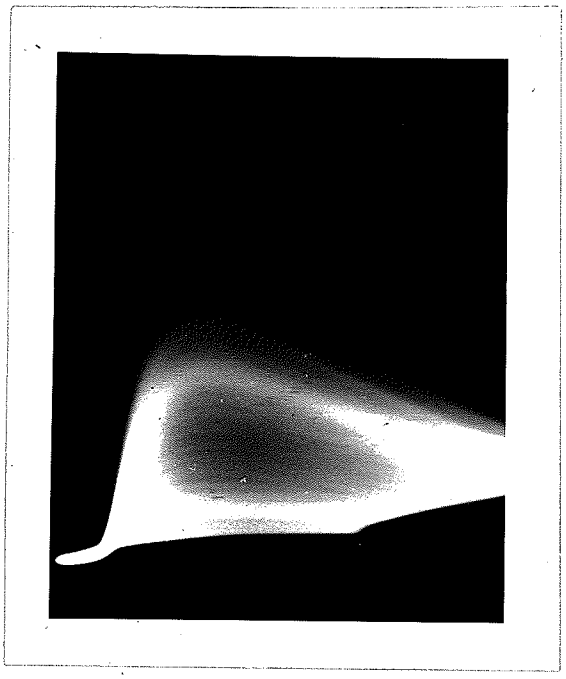

PLATE 1.

Oscillogram of cobalt 60 spectrum.

4.3 The gamma rays of iodine 131.

Iodine 131 has been studied extensively in recent years mostly as regards its disintegration scheme. The gamma ray energies have been measured by Metzger and Deutsch (27) and there is general agreement between their values and those obtained with the scintillation spectrometer (28,29). In the present work iodine 131 was studied primarily because of the range of values of gamma ray energy from 30 KeV to approximately 600 KeV. This permitted the examination of the operation of the spectrometer in an energy region where the photoelectric cross-section of iodine in the crystal is much greater than its value for either of the cobalt 60 gamma rays. (See Figure 1.)

Study of the photolines due to these gamma rays permitted an accurate measurement of the performance of the spectrometer and the value of changes in any part of the equipment could be quickly assessed. The linearity of the spectrometer was checked accurately and, as has already been pointed out, this is now considered to hold up to energies of at least several MeV and down to energies of 10 KeV or thereabouts (X-rays).

A pulse height distribution curve for iodine is shown in Figure 12, and on the same diagram a plot of pulse height v. gamma ray energy is given. It can be seen that the latter is, at all points, within 1% of the value required by a linear relationship and this is within the experimental error in determining the position of a peak.

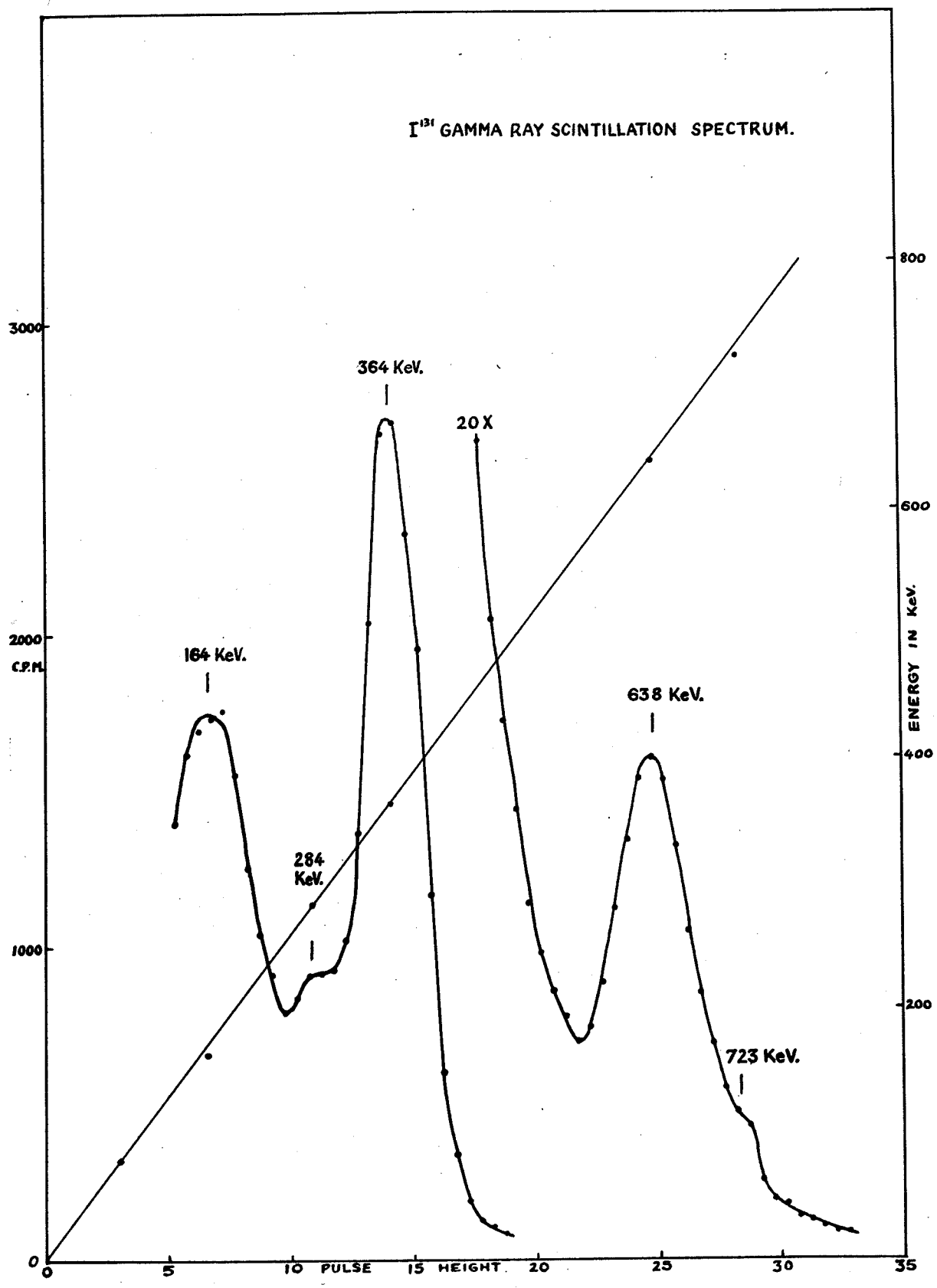
I¹³¹ GAMMA RAY SCINTILLATION SPECTRUM.
3000
2000
C.P.M.
1000
0
800
600
400
200
ENERGY IN KeV.
364 KeV.
20 X
164 KeV.
284 KeV.
638 KeV.
723 KeV.
0
5
10
15
20
25
30
35
PULSE HEIGHT

FIGURE 12.

The 364 KeV line is very intense and is well seperated from other prominent lines. Thus it can be used to great advantage for calibration purposes and in the present investigations has been so used. In addition, the 80 KeV gamma ray is also prominent, and is very useful in the low energy region while for still lower energies the K-ray from Xenon, resulting from internal conversion, is prominent and most useful. Its energy is 29.0 KeV.

A comparison of the latest scintillation spectrum and that appearing in The Review of Scientific Instruments (26) emphasises once again the improvements in resolution which have been achieved.

An oscillogram of the spectrum in Plate 2A shows clearly the intense 364 KeV line with the 164 KeV and 80 KeV lines below it, while Plate 2B shows the high energy 638 KeV line. Plate 2C is an oscillogram taken by the beam intensity modulation method, the peak on the right being the 364 KeV line.

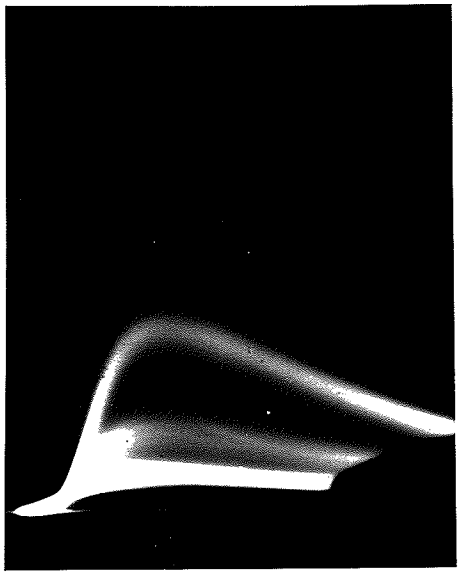

PLATE 2A.

Oscillogram of iodine 131 spectrum.

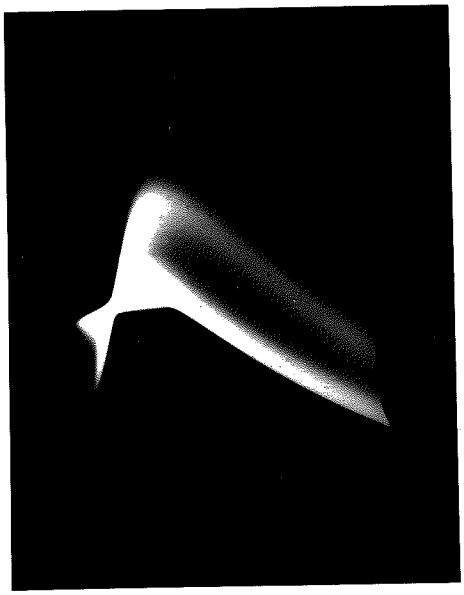

PLATE 2B.

Oscillogram of iodine 131 spectrum.

(high energy region)

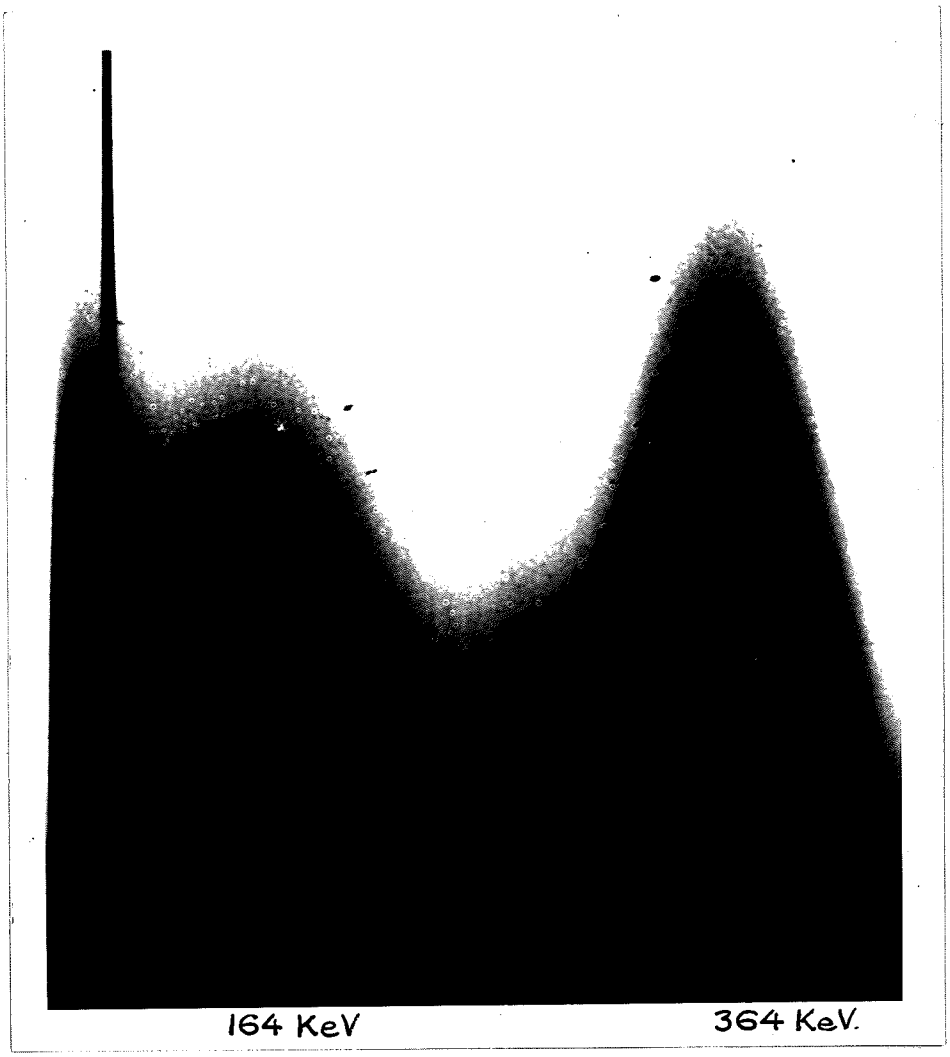

PLATE 2C.

Oscillogram of Iodine 131 spectrum.

(Intensity modulation method of display.)

4.4. The gamma rays from a polonium beryllium neutron source.

The study of the gamma rays from a polonium beryllium neutron source originally started out as a study of the neutron energy distribution (26). However, the gamma radiation proved to be stronger than anticipated so that a study of the gamma ray energy distribution was undertaken.

The gamma radiation arises from the nucleus resulting from the reaction

$$Be^{9} + \alpha \rightarrow C^{12*} + n ,$$
$$C^{12*} \rightarrow C^{12} + \gamma .$$

The distribution showed a very prominent peak which appeared to be due to a high energy gamma ray (See Figure 13A). This was identified as a pair production line and was the first demonstration of this phenonenon in a scintillating crystal (30). It was considered desirable to calibrate the spectrometer in this energy range with a source giving known high energy gamma rays, and thorium appeared to be an obvious choice. The thorium spectrum contains a prominent 2.62 MeV component due to thorium C'' . This might be expected to give a pair production peak at 1.60 MeV on an energy scale, and such a peak was obtained. The pair production peak in the neutron source spectrum occurred at 3.45 MeV on this scale, corresponding to a gamma ray energy of 4.47 MeV. A further very weak pair production peak was obtained at 6.2 MeV on the energy scale corresponding to a gamma ray of 7.2 MeV. These results

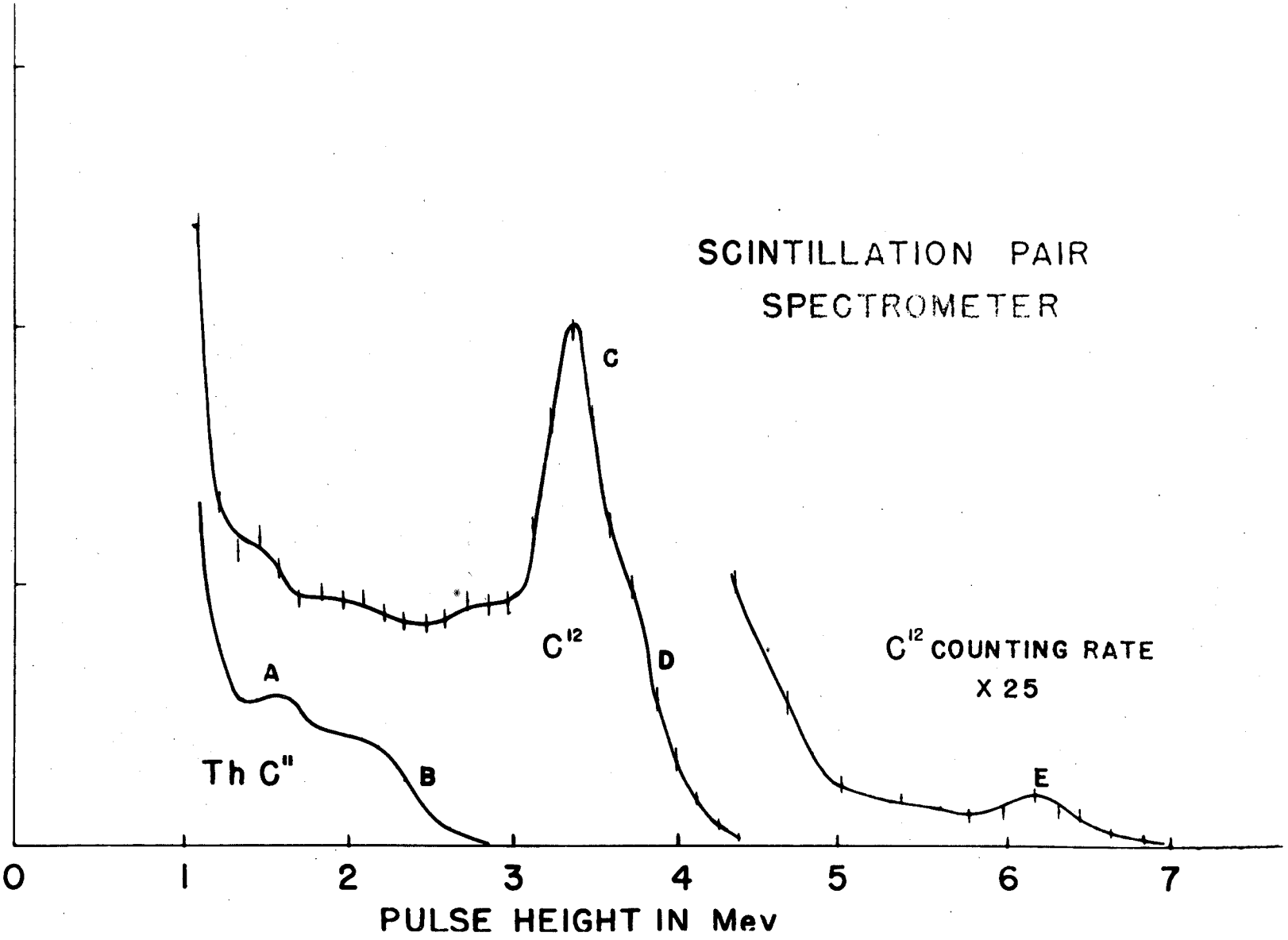
SCINTILLATION PAIR
SPECTROMETER
COUNTING RATE
3
2
1
0
1
2
3
4
5
6
7
PULSE HEIGHT IN Mev
A
B
C
D
E
Th C''
C12
C12 COUNTING RATE
X 25

FIGURE 13A.

are in agreement with those of Bradford and Bennett (31) obtained from a study of the neutron groups. No gamma rays of any appreciable intensity were found in the 2-4 MeV region.

A resolution on the 3.45 MeV pair production line of about 8% was obtained.

A recent scintillation spectrum of the same source is shown in Figure 13B. The polonium content had been much reduced by decay for a period of almost two years which amounts to some five half-lives. The counting rate was consequently much lower and the presence of impurity, which was suspected in the source originally, was confirmed by the considerable alteration in the shape of the curve during the two-year period. In the curve shown there are two humps on the high energy side of the pair production peak, and these can be attributed to the capture of one and of two positron annihilation quanta. The separations between the pair production peak and the humps should be 0.51 MeV and 1.02 MeV respectively. These intervals have been marked out on the spectrum plot and show that subsidiary peaks occur at the anticipated places. The estimated resolution on the 3.45 MeV peak is between 5% and 6%.

Plate 3 shows an oscillogram of the spectrum. The 3.45 MeV pair production peak is visible at the top of the spectrum, and in the lower half gamma rays due to radium impurity in the source are in evidence.

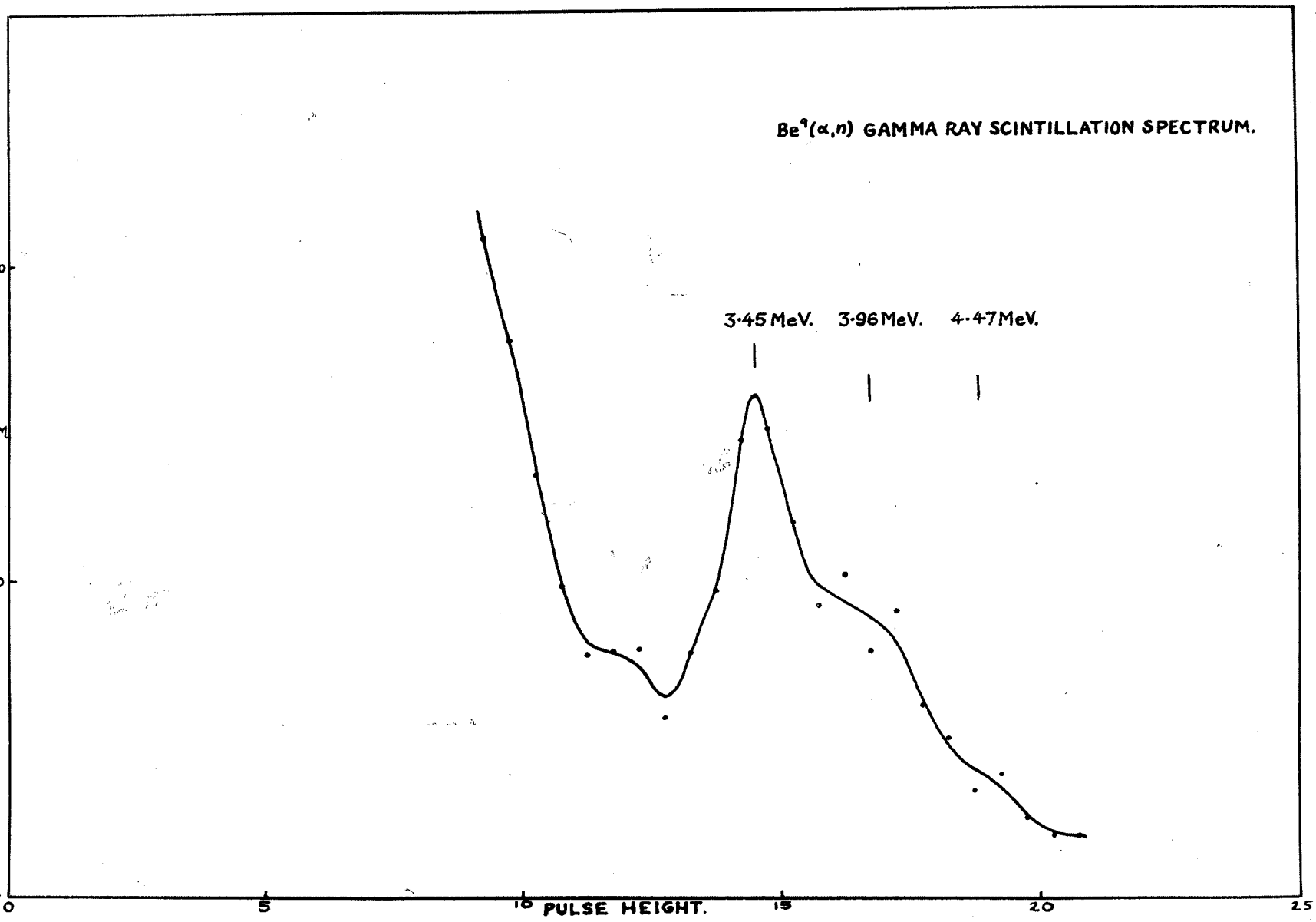
Be⁹(α,n) GAMMA RAY SCINTILLATION SPECTRUM.
3·45 MeV.
3·96 MeV.
4·47 MeV.
C.P.M.
20
10
0
0
5
10
15
20
25
PULSE HEIGHT.

FIGURE 13B.

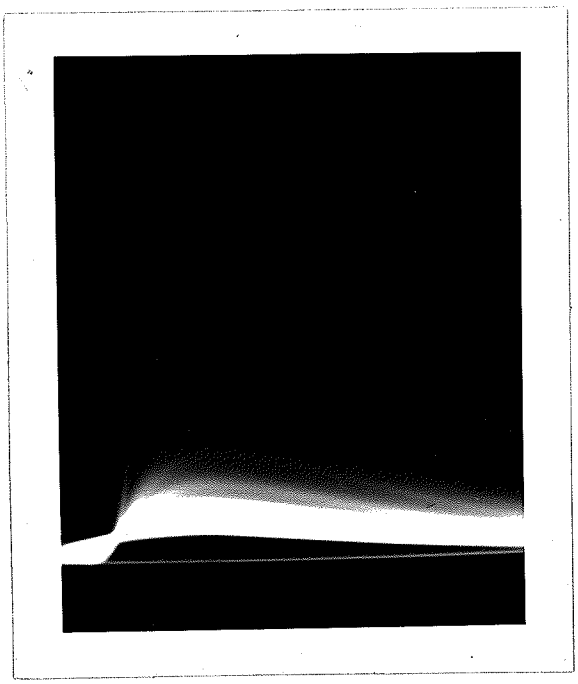

PLATE 5

Densitometer of Fe-Be spectrum.

4.5. The gamma rays of thorium.

As has already been mentioned, a thorium source, in equilibrium with its daughter products, was used for calibration purposes in the study of the gamma rays from a polonium-beryllium neutron source. The gamma ray spectrum was plotted in some more detail so that it would be available for reference purposes. (See Figure 14).

The 2.62 MeV gamma ray from thorium C'' gave a prominent pair production peak at 1.60 MeV and peaks were also obtained at points approximately 0.5 MeV and 1.0 MeV higher up on the energy scale corresponding to the capture of one annihilation quantum or of both. In addition, a Compton edge was apparent on the higher energy side of the peak corresponding to the capture of one quantum, and distorted it considerably. The Compton cross-section in this energy region is still very considerable, as it falls off approximately as the reciprocal of the gamma ray energy, and the pair production cross-section has not reached a very large value, although it increases rapidly with energy. It is to be expected, therefore, that the Compton contribution will be quite considerable.

Plate 4 shows the oscillogram of the spectrum and its resemblance to the distribution curve of Figure 14 is apparent.

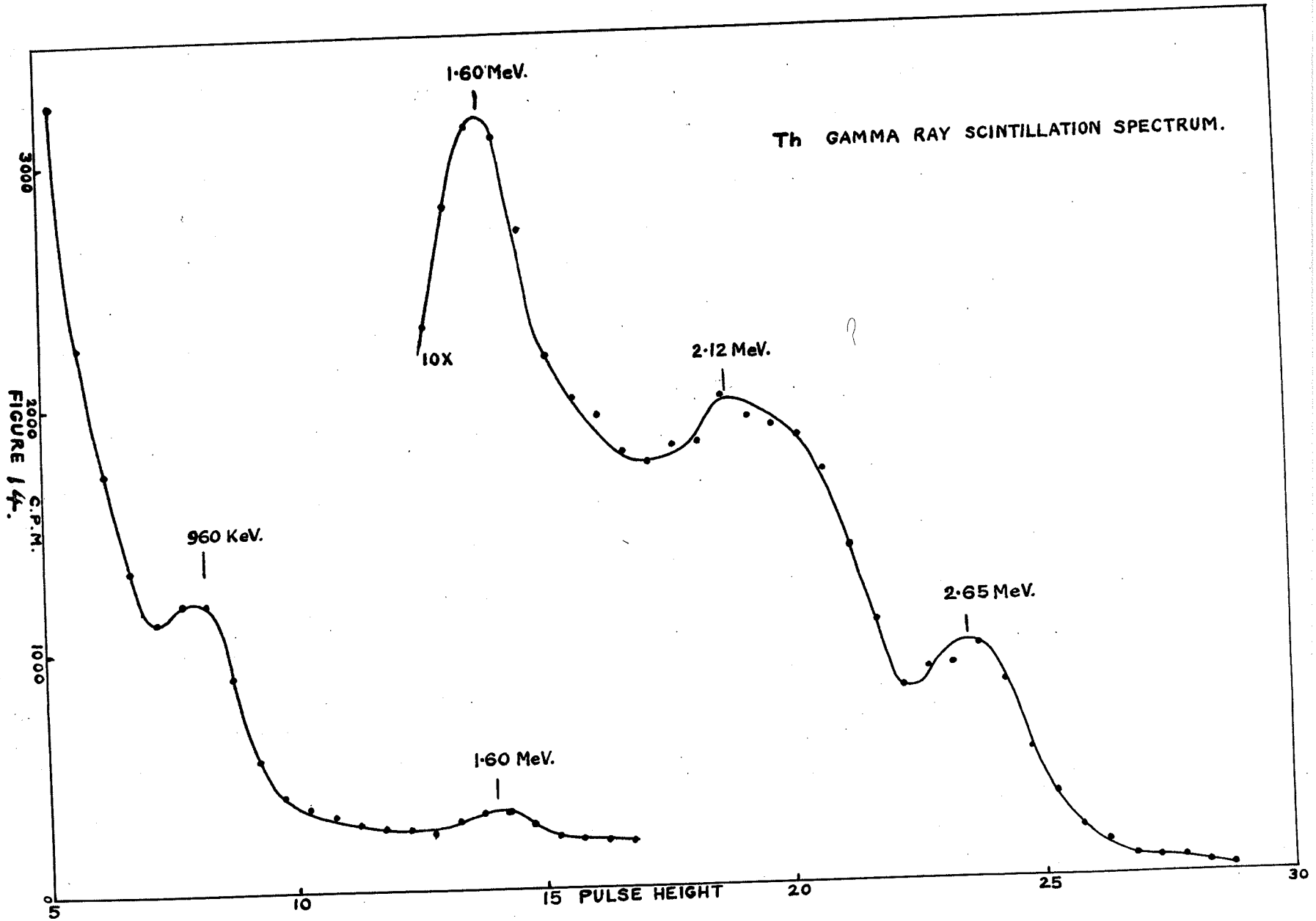
Th GAMMA RAY SCINTILLATION SPECTRUM.
1·60 MeV.
10X
2·12 MeV.
960 KeV.
2·65 MeV.
1·60 MeV.
3000
2000
1000
0
C.P.M.
5
10
15
20
25
30
PULSE HEIGHT

FIGURE 14.

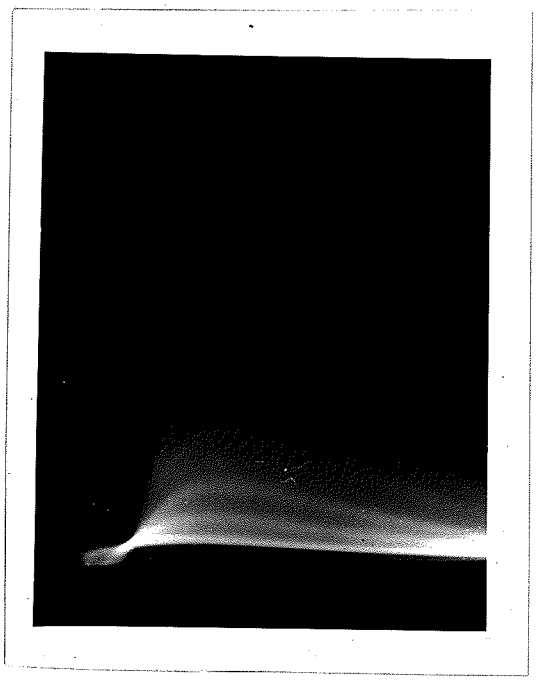

PLATE 4

Oscillogram of thorium spectrum

4.6. The gamma rays of radium.

As with thorium it was considered of interest to plot the gamma ray scintillation spectrum of radium in equilibrium with its daughter products, and this is shown in Figure 16.

A strong line was obtained at 0.62 MeV (photo-electric line), and weaker lines (also photoelectric) were obtained at 1.13, 1.46, 1.81, 2.23 and 2.42 MeV. All of these gamma rays are emitted by RaC.

The values found here agree reasonably well with those found by other workers. (32-37)

Plate 5 shows the oscillogram of the spectrum. Note the resemblance to the lines showing in the Po-Be neutron source spectrum (Plate 3).

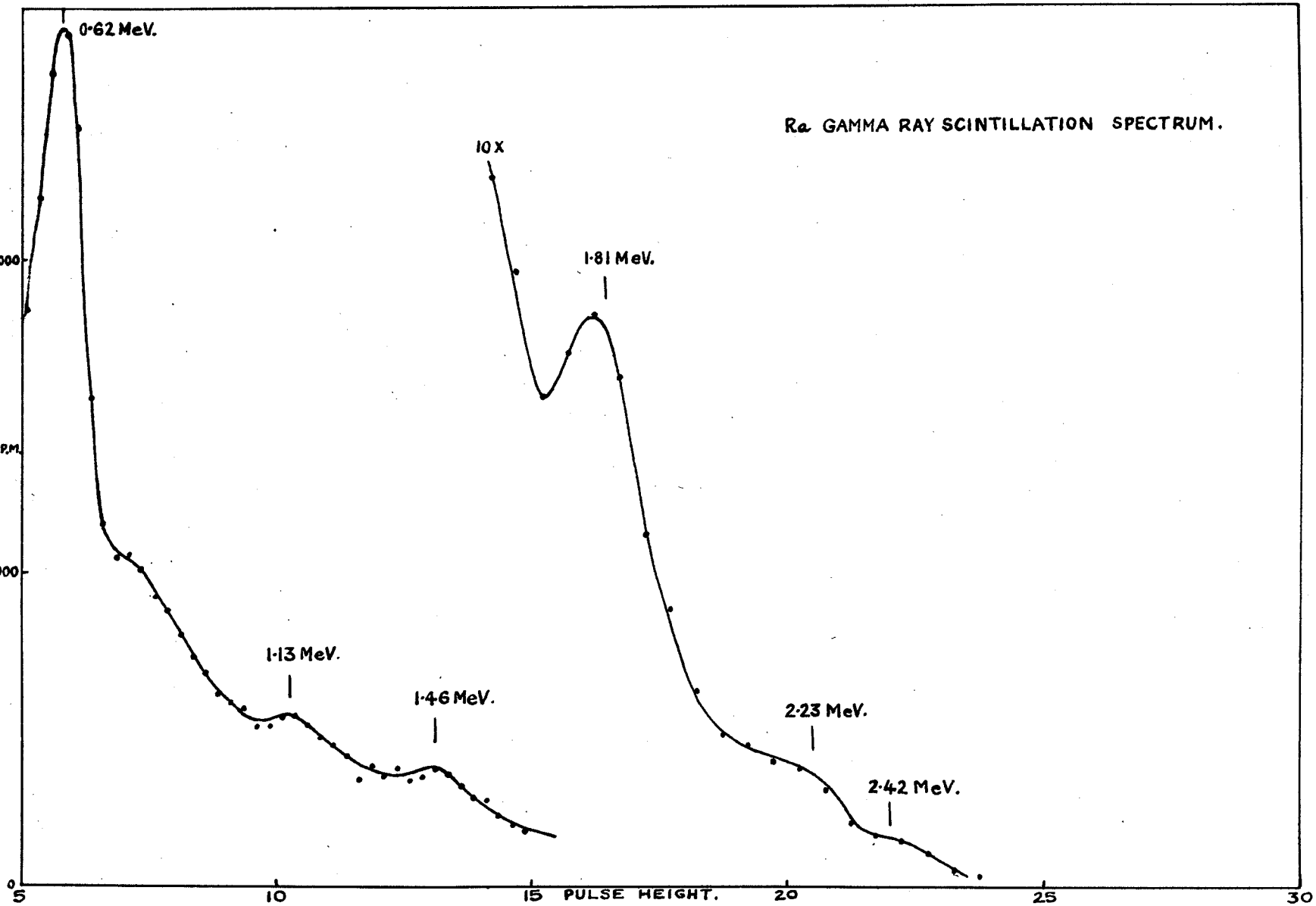
Ra GAMMA RAY SCINTILLATION SPECTRUM.
0·62 MeV.
10 X
1·81 MeV.
1·13 MeV.
1·46 MeV.
2·23 MeV.
2·42 MeV.
C.P.M.
2000
1000
0
5
10
15
20
25
30
PULSE HEIGHT.

FIGURE 15.

PLATE 8.

Oscillogram of radium spectrum

4.7. The neutron capture gamma rays of aluminum.

Artificially produced radioactive isotopes are studied very widely at the present time, chiefly because of their availability. With the construction of nuclear piles in several countries, the production of radioactive isotopes is now a commonplace procedure and is organised on a large scale. Most of the radioactive isotopes are produced by bombardment of stable isotopes with thermal neutrons and, an excess energy being available equal to the binding energy of the last neutron in the product nucleus, the latter becomes de-excited by the emission of what is called the neutron capture gamma radiation. The study of this radiation, which is emitted within a very short time of the capture of the neutron, has in the past been limited almost entirely to laboratories with pile facilities available. It was felt that the scintillation spectrometer with its high gamma ray efficiency might permit the study of capture gamma rays by using the relatively low neutron fluxes obtainable from fabricated neutron sources, e.g. radium - beryllium or polonium-beryllium. For this reason certain investigations were undertaken to ascertain the value of the scheme (38) and in this thesis a report is made on the capture gamma rays of aluminum.

Owing to the gamma radiation from the neutron source itself, precautions had to be taken to minimise this, without, at the same time, reducing the radiation from the aluminum to

a level too low for observations to be made. The arrangement at present in use is to shield the scintillating crystal from the neutron source (a 400 millicurie polonium beryllium source was used here) by a lead cylinder about 6 inches long and 1½ inches in diameter. The target, an aluminum block about 3 inches in diameter and 3 inches high had a recess cut in it so that it fitted over the scintillating crystal. A cylindrical block of paraffin wax with suitable holes cut in it surrounded the crystal, target, lead shield and neutron source, and served the purpose of thermalising the neutrons.

In the measurement of the gamma radiation a background determination was first made with the neutron source, paraffin block and lead cylinder all in their normal positions. The target was then placed in position and a further run made. The differences between corresponding counts were taken to be the counts due to the target, and this is what has been plotted in Figure 16.

Actually this method of arriving at the counts due to the target is not quite correct for, in taking the background count, the target does not surround the crystal and the shielding effect which it has when it is in position is not felt. Thus the background count is higher than it should be, and in the lower energy region has been found on occasion to be greater than the background and genuine signal. This gives a meaningless curve in the particular energy region and

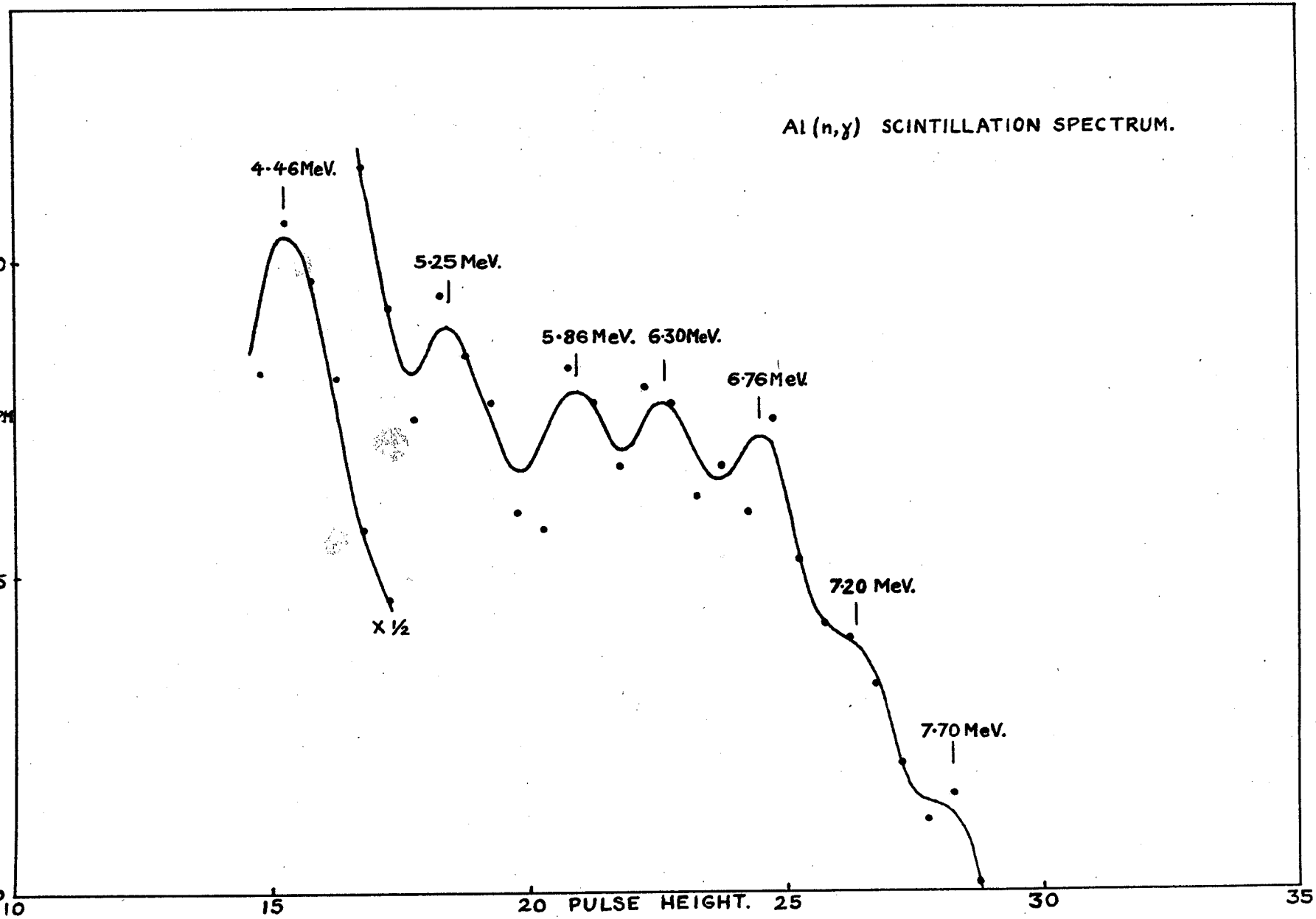
Al (n,γ) SCINTILLATION SPECTRUM.
4·46MeV.
5·25 MeV.
5·86 MeV.
6·30MeV.
6·76MeV.
7·20 MeV.
7·70 MeV.
X ½
10
5
0
CPM
10
15
20
PULSE HEIGHT.
25
30
35

FIGURE 16.

interpretations have been made only in the upper energy region, from about 5 MeV upwards.

To interpret the results it must be appreciated that one gamma ray may give three peaks, as with the 4.47 MeV neutron source gamma ray or the 2.62 MeV thorium gamma ray, corresponding to the gamma ray energy less 1.02 MeV, and the gamma ray energy less 0.51 MeV and the full gamma ray energy. As will be seen on examination of the spectrum this makes the interpretation very difficult especially as the peaks obtained were roughly at 0.5 MeV intervals.

On the assumption that the pair production peak is considerably stronger than the subsidiary peaks where one or both annihilation quanta are captured, there is some justification for taking the peaks at 5.25 MeV, 5.86 MeV, 6.30 MeV and 6.76 MeV as being pair production. These would correspond to gamma rays of energies 6.27, 6.88, 7.32 and 7.78 MeV. The humps at 7.20 and 7.70 MeV are probably the subsidiary peaks belonging to the 6.76 MeV peak.

Kinsey, Bartholomew and Walker (18) report gamma ray energies of 7.724, 7.34, 6.98, 6.77, 6.61, 6.50, 6.33, 6.22, 6.13 MeV as well as many others of lower energy. Of these the 7.724 MeV line is the strongest and the lines at 6.77, 6.33 and 6.13 MeV are of medium intensity, the remainder being weak. While it could be said that there is some correlation between the results of the two methods, the

resolution of the scintillation pair spectrometer is not sufficiently high to separate lines so close together as those of aluminum. However, the end-point of the spectrum seems to be very well defined and if one makes allowance for the statistical spread, a reasonably accurate figure for the maximum gamma ray energy is obtained. In the present experiment this agrees remarkably well with the value of Kinsey et al, although the relative intensities in the two methods do not appear to agree.

It is felt that, while the scintillation pair spectrometer in its present form is not adequate to show up the fine detail of the average capture gamma ray spectrum, it should, nevertheless, prove of considerable value in determining the maximum gamma ray energy. This gamma ray is, in many cases, that associated with the transition to the ground state. Thus it can give the binding energy of the last neutron in the product nucleus.

The pair production peak of the gamma rays of the neutron source, which occurs at 3.45 MeV was used for calibration purposes. A photograph of the pulse height distribution on the cathode ray oscillograph showed the presence of radium impurity in the source.

The neutron source had a flux of 10^6 neutrons per second, the average energy of the neutrons being 4.1 MeV. The ratio of RaD (in millicuries) to Be (in milligrams) was 1/15. The gamma radiation background was that due to 0.22 millicuries of radium.

5. THE COINCIDENCE TECHNIQUE.

The application of coincidence techniques to experiments in nuclear physics has been discussed very thoroughly by Dunworth (39). In 1924 Bothe and Geiger used the technique to study the Compton effect. In 1930 it was used for cosmic ray studies, and in 1935 Bothe and von Baeyer (40) used it for the detection of two particles emitted simultaneously, thus initiating time-correlation studies. This technique has since been used by a very large number of workers and has led to the elucidation of the decay schemes of many radioactive isotopes, this being the principal application.

Dunworth shows that, for a given accuracy f, the time T of coincidence counting approaches a limiting value as the source strength is increased and no great advantage is obtained by increasing the source strength beyond the value where the number of disintegrations per second is 1/2t, where t is the resolving time of the equipment. For such a source strength the accidental coincidence counting rate is equal to the genuine coincidence counting rate.

The efficiencies of the counters do not enter into the expression for the optimum source strength. However, the time taken for an experiment of a certain accuracy depends on the reciprocal of the product of the net efficiencies of the counters, and it also depends directly on the equipment resolving time. The net efficiency is defined as the efficiency per unit solid angle integrated over a sphere. In other words

it includes a factor for the solid angle subtended by the counter at the source.

Besides investigating the time-correlation of different particles or radiations emitted by a disintegrating nucleus, Dunworth was able to measure the net efficiencies of counters by using sources with known simple decay schemes. He was also able to measure the half-lives of short lived radioactive elements (in the region 10^{-7} to 10^{-3} second) by introducing a variable resolving time into the circuit (41).

Dunworth used Geiger-Muller counters and found experimentally the relationship between the energy of a gamma ray and the detection efficiency of the counter for that gamma ray. He proposed this as a method of estimating gamma ray energy.

In the present experiments a high net detection efficiency (5-20%) for gamma rays was achieved, whereas Dunworth's values ranged from 0.05% to 0.5% depending on the gamma ray energy. Thus it was possible to obtain a count of a certain accuracy in approximately 10^{-3} of the time required by Dunworth, assuming that a source of optimum strength was used. As an example, the time taken for a count of 3% accuracy, using a Geiger-Muller counter, with a net efficiency assumed to be 0.1% and a resolving time of 1 microsecond, is 35 minutes while, for a scintillation counter with a net efficiency of, say, 5% and the same resolving time, the count-

ing time is less than one second. Thus it is seen that with the scintillation counter much time is saved and it has been found unnecessary, in practice, to use a source as strong as the optimum. A ratio of genuine counts to accidental counts of about 10:1 has been maintained which would correspond to a source strength about 1/10 of the theoretical optimum.

Although a Geiger-Muller counter may be made to operate with a resolving time as low as 0.2 microsecond, the counter is inactive for a much longer period (100 microseconds or more) after the detection of a particle or quantum. Thus if it had a much higher efficiency e. g. in the detection of beta particles, it would not be advantageous to use the optimum source strength, as many of the counts would be lost due to the occurrence of nuclear events during the "dead" periods. The pulse height analysing equipment associated with a scintillation counter may have a "dead" time of a few microseconds so that, considering its high detection efficiency, the weaker-than-optimum source is highly desirable. Sources estimated to be 1 to 10 microcuries have been used in the experiments described.

The scintillation counter has a further advantage viz. the fact that it can be used as a gamma ray spectrometer. Thus it is possible to effect at least a partial separation of the pulses due to gamma rays of different energies and coincidences between the different gamma rays can be studied. Without this ability to separate the gamma rays of different energies, only isotopes with simple decay schemes can be

studied with reasonable hope of unambiguous results. Until the advent of the scintillation spectrometer the most successful method of separation of gamma rays of different energies was the absorption technique. This was applied extensively in coincidence experiments.

The equipment layout for the coincidence experiments is shown in Figure 17A. It consists essentially of two gamma ray scintillation spectrometers, although one of these may be operated as a beta particle spectrometer by using an anthracene crystal to detect the beta particles (anthracene is relatively inefficient for the detection of gamma rays). Two photomultiplier tubes with crystals attached as in Figure 17B are mounted with the crystals close together in a light-tight box, a picture of which is shown in Plate 6. The source is placed between the crystals and the solid angle subtended by a sodium iodide crystal (1 inch diameter cylinder, 1 inch long) is estimated to be approximately 3 steradians. For beta particle detection the source is mounted between two small anthracene crystals which are placed on the end of one photomultiplier and an aluminum plate is placed between the source and the other (gamma ray detecting) crystal to prevent beta particles from reaching it. The purpose of using two crystals round the source for beta detection is to obtain a large solid angle for beta particle collection and thus minimise scattering effects at the crystal surface close to the source.

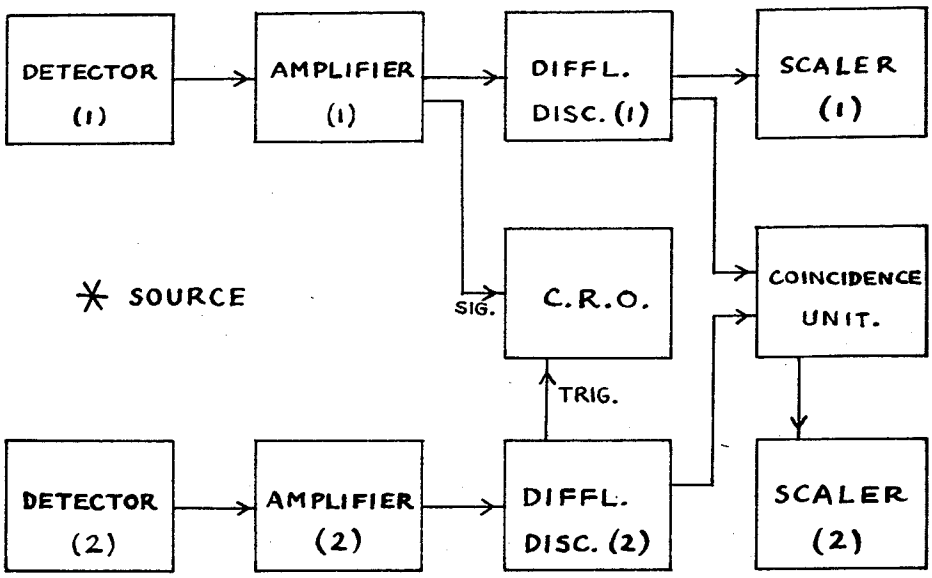

(A) COINCIDENCE SPECTROMETER BLOCK SCHEMATIC.

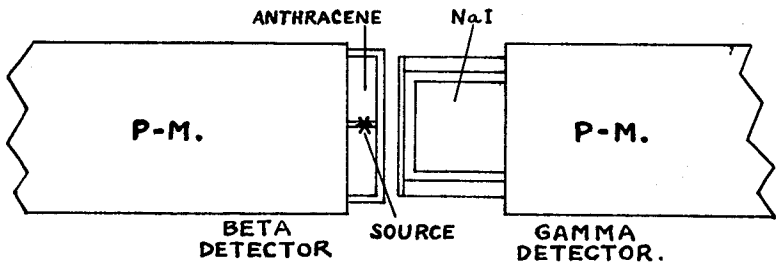

(B) CRYSTAL AND SOURCE ARRANGEMENT FOR BETA-GAMMA COINCIDENCES.

FIGURE 17.

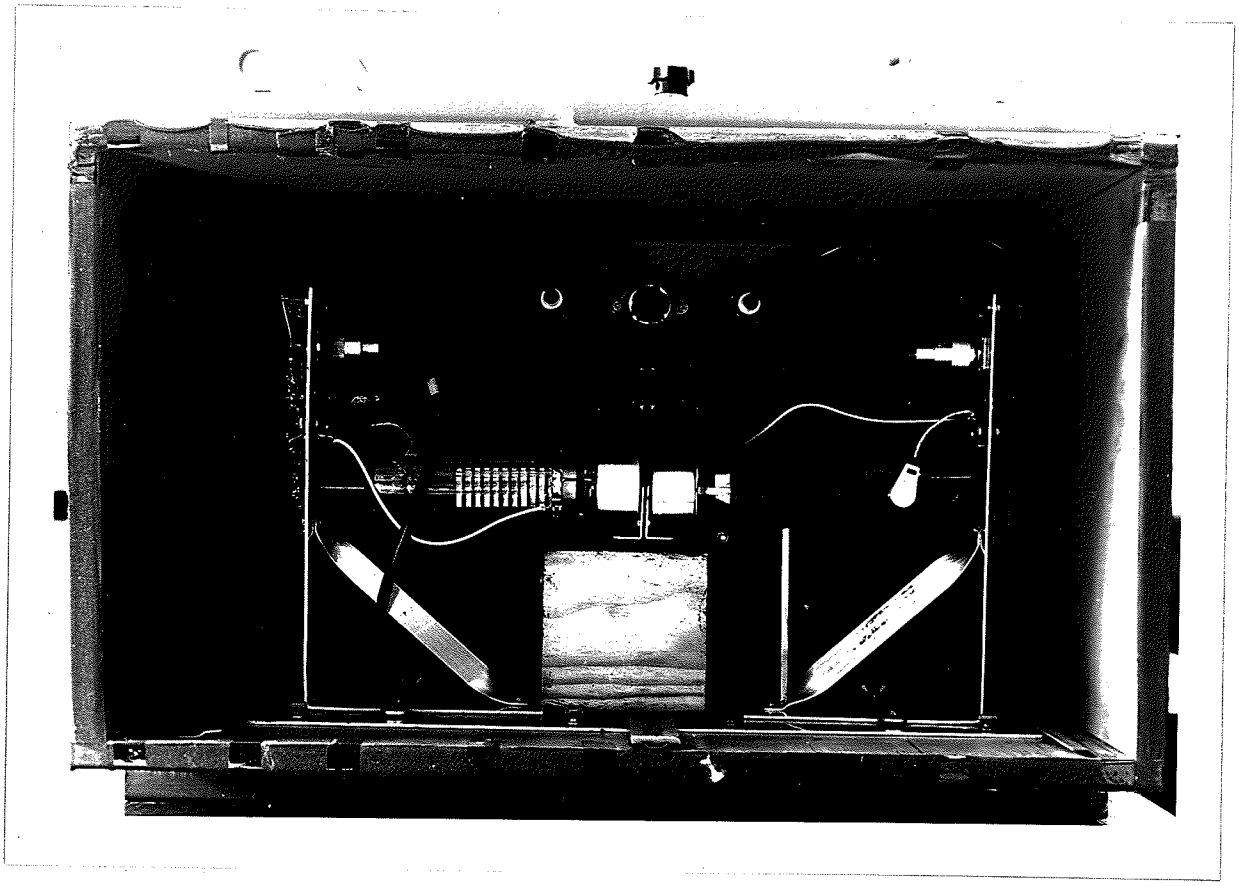

PLATE 6.

Scintillation counters mounted for coincidence experiments.

A cathode follower output is provided for each photomultiplier and these feed into two linear amplifiers of the type shown in Figure 8. The amplifiers feed into two pulse height analysers shown in Figures 6 and 7, and the outputs of the analysers go to a coincidence unit type 1036A (A.E.R.E.). Scalers are used to record the counts not only of coincidences but also of pulses in the two spectrometer circuits.

The 1036A coincidence unit has not so far been described, so a brief explanation of its facilities will be given. It consists of three identical channels each of which may be triggered by pulses of amplitude greater than a pre-selected value. Two channels are used for ordinary coincidences and three are used for triple coincidences. The outputs from the channels are fed to a mixer unit which gives out pulses only when a certain set of conditions, selected on a switch, is met. These conditions are:-

(1) two coincident pulses received from the first two channels

(2) three coincident pulses received

(3) two coincident pulses received from two channels and no pulse from the third (anti-coincidence)

(4) one pulse received from one channel and no pulse from the third (anti-coincidence).

For the investigation of decay schemes, which involves beta-gamma and gamma-gamma coincidence studies, condition (1) is normally applied although there may be occasions on which

the application of condition (2) might give additional or less ambiguous information. Conditions (3) and (4) are generally used for special purposes.

In addition each of the channels has included in the circuit a delay line by which pulses may be delayed by up to 1 microsecond. This is useful for an experimental determination of the accidental coincidence counting rate, as a sufficiently long delay in one channel will eliminate genuine coincidences, assuming no metastable states to be present. The resolving time of the mixer stage is variable and in the experiments performed a value of 0.3 microseconds has been found satisfactory. When using sodium iodide (activated) as a scintillator, the light output pulse has a rise time of approximately 0.2 microseconds. The use of a resolving time much less than this results in an uncertainty as to whether or not a genuine coincidence will be counted, so that the longer one is to be preferred.

In a coincidence experiment the scintillation spectrum is plotted for one of the two channels first of all. This channel is labelled (2) in Figure 17A, and will be referred to as channel (2) in the description following. From this the pulse height analyser bias levels necessary to select pulses due mainly to a gamma ray, which it is desired to put in coincidence with the rest of the spectrum, are determined. The analyser levels are set accordingly and the coincidence

experiment proper is carried out. The whole spectrum is scanned with the channel labelled (1) in small steps and the counting rates determined in the normal way. At the same time, the pulses from this channel are passed into the coincidence unit together with the pulses selected from channel (2) (mainly those due to a gamma ray of a certain energy), and the coincidence counting rate is determined for each step. Thus the total gamma ray spectrum and the coincidence spectrum are obtained.

If the gamma ray, chosen in channel (2), is in coincidence with all other gamma rays in the total spectrum then the coincidence spectrum will have the same shape as the total spectrum except in the region of the chosen gamma ray, where there will be fewer coincidence counts as a gamma ray cannot be in coincidence with itself. Since differences between the shapes of two curves are somewhat difficult to detect especially on those parts of the curves where the counting-rate is low, it has been found advantageous to plot the ratio of the coincidence counting rate to the total counting rate. Then this ratio will have a constant value in regions where the gamma rays are in coincidence and will be reduced in value where the gamma ray of channel (2) is not in coincidence with the gamma ray of channel (1). A dip in the "ratio" curve, therefore, indicates a lack of association between the gamma ray selected in channel (2) and a gamma ray in channel (1).

Some typical decay schemes are shown in Figure 18 together with the form of the "ratio" curve to be expected for each decay scheme. The transition from one value to another in the ratio curve is sharp or gradual depending on the resolving power of the spectrometer. In practice it is impossible to separate completely the pulses due to the different gamma rays. There is always a certain amount of overlapping of the distribution curves and this causes the ratio curve not to change very sharply from one level to another. It rarely reaches the zero level due to this spreading out of the pulses over the pulse height scale.

There is also the question of accidental coincidences to be considered. If the counting rates in the two channels are respectively N_1 and N_2 counts per second, and if the resolving time of the equipment is t seconds, then the accidental counting rate is $2 t N_1 N_2$ counts per second. This accidental counting rate expressed as a fraction of the counting rate in channel (1) is $2 t N_2$. But t and N_2 are constant for a particular experiment, hence the "ratio" curve need only have its zero changed to correct for the accidentals.

An alternative or supplementary method of recording the results is to use a cathode ray tube to display the coincidence spectrum and the full gamma ray spectrum in turn and a camera to integrate the effect over a suitable period of time. To display the coincidence spectrum the output pulses from the

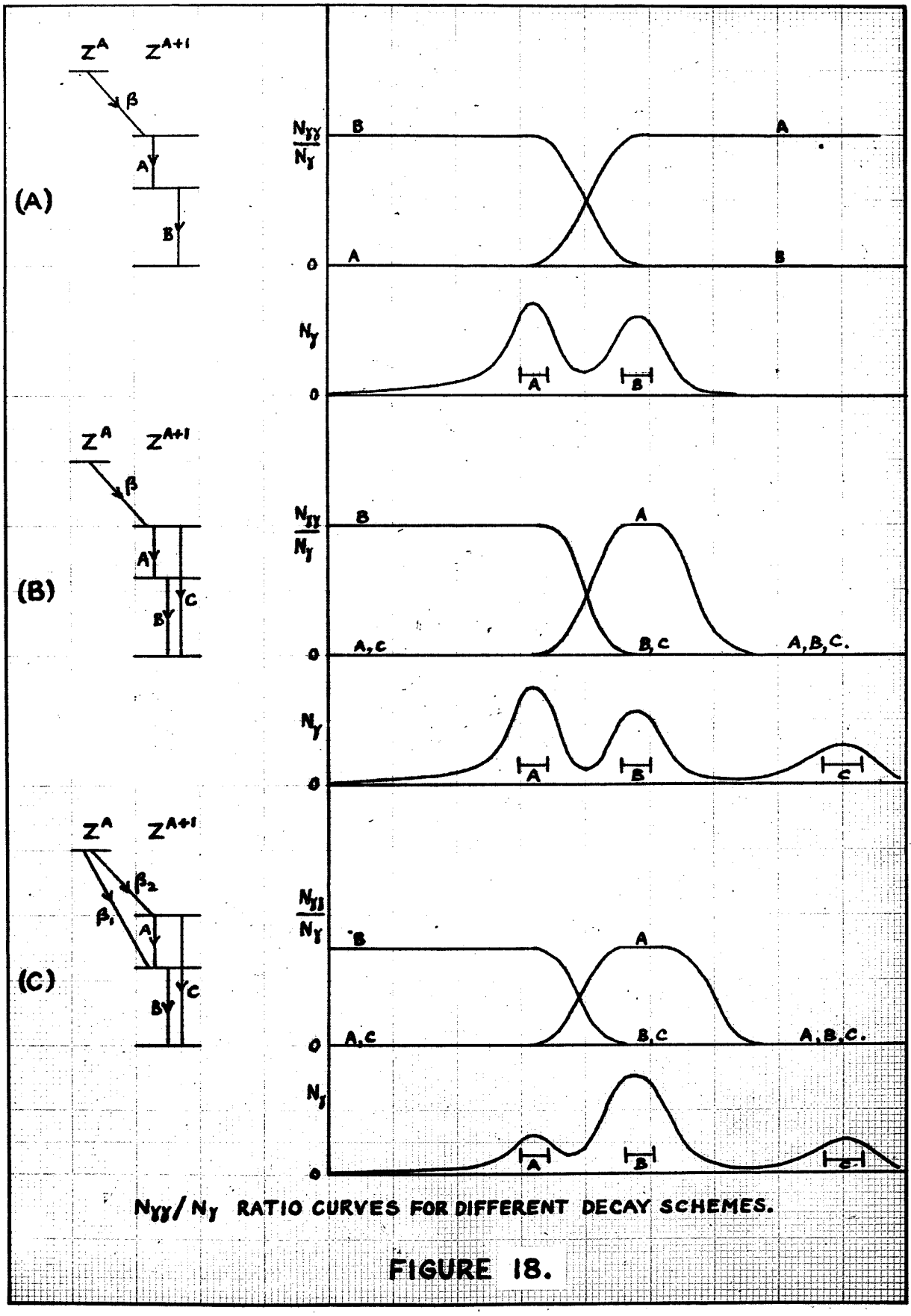

$N_{\gamma\gamma}/N_\gamma$ RATIO CURVES FOR DIFFERENT DECAY SCHEMES.

FIGURE 18.

NOTE:- The horizontal lines, marked A, B, etc. on the N_γ curves represent the gates fixed in channel (2) for the coincidence curves marked A, B, etc. respectively.

pulse height analyser in channel (2) are used to trigger the time-base of the oscilloscope, and the pulses in channel (1) which are in coincidence are displayed on the screen with their peaks close to the beginning of the sweep. This method does not show up slight differences in the shapes of the spectra and hence is not of much use except where simple decay schemes are being studied, or where the high energy portions of a spectrum are being studied. In the latter case there is no mixing of pulses due to low energy gamma rays with those due to the high energy gamma rays, hence differences in the shapes of the spectra are more obvious.

As a matter of interest, the photographic method provides information at the same time as to the accidental counting rate, for accidental coincidence pulses are distributed evenly across the screen. Further, if a meta-stable state with a half-life in the region of 1 to 10 microseconds is formed, the density of pulses arising from the decay of this state is highest at the beginning of the sweep and falls off exponentially towards the right hand side.

Two examples of coincidence spectra obtained for iodine 131 are shown in Plates 7A and 7B. In Plate 7A the spectrum in coincidence with the 163 KeV gamma ray is shown on the left, while the full spectrum is shown on the right, for calibration purposes. Similarly in Plate 7B the spectrum in coincidence with the 635 KeV gamma ray is shown on the left

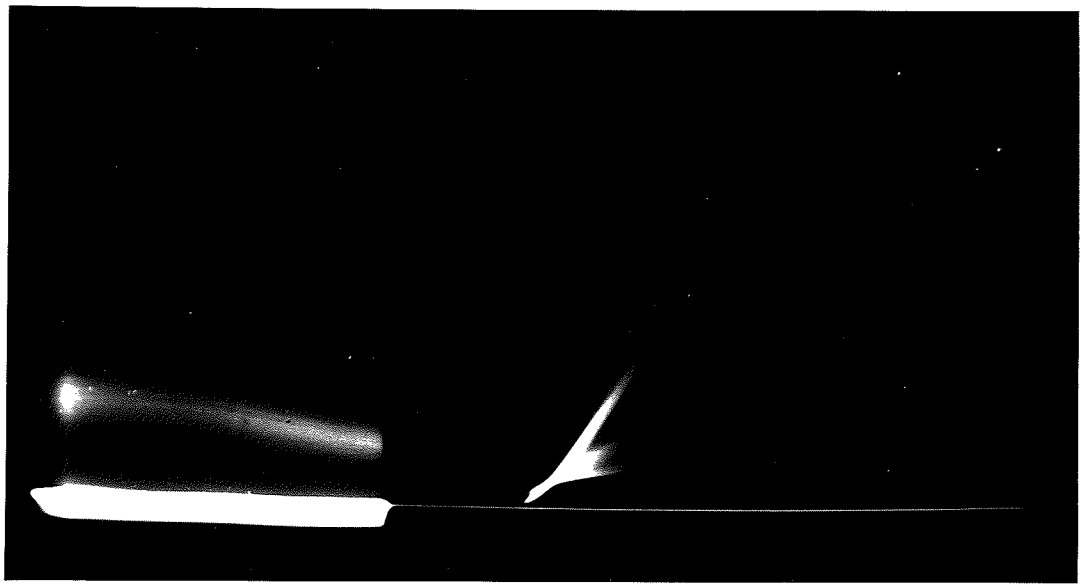

PLATE 7A.

Iodine 131 spectrum in coincidence with 163 KeV gamma ray (left). Full spectrum (right).

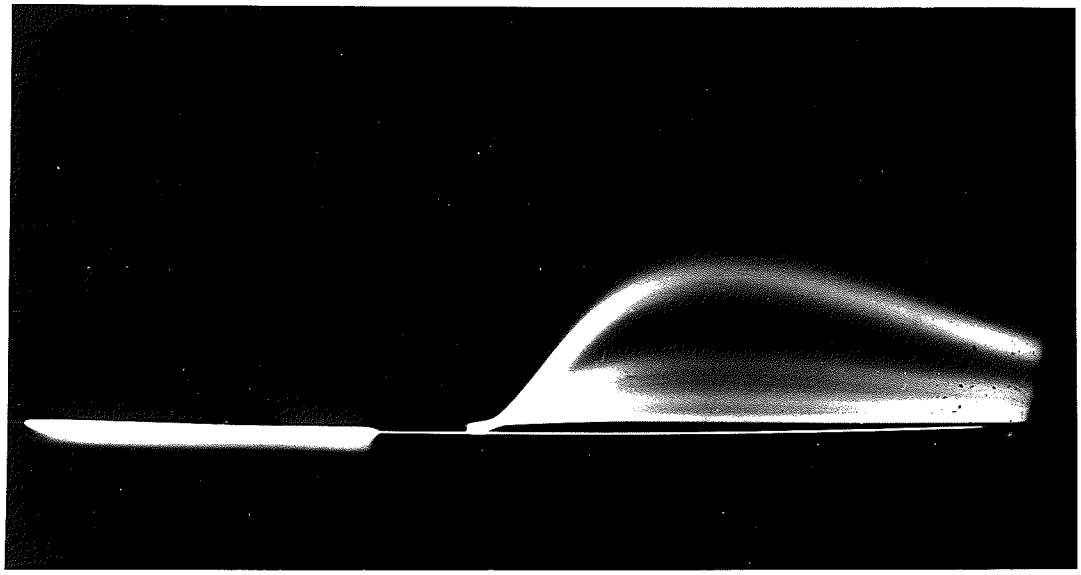

PLATE 7B.

Iodine 131 spectrum in coincidence with 635 KeV gamma ray (left). Full spectrum (right).

with a calibration spectrum on the right. It will be noticed that the rising fronts of the pulses in the coincidence spectrum are lost due to delay in the arrival at the cathode ray oscilloscope of the triggering pulse which is generated by the pulse height analyser.

Where scalers are used with the coincidence equipment the existence of a meta-stable state is shown up by a higher than normal coincidence counting rate when a delay longer than the resolving time is inserted in one of the channels. The normal coincidence counting rate with the delay is, of course, the accidental counting rate and should agree with the rate calculated from the formula given above.

Plate 8 shows the arrangement of the rack-mounted units in the coincidence equipment. In the middle of the picture a beta particle spectrometer equipped for beta-gamma coincidence counting is shown with the field current control panel in the right background.

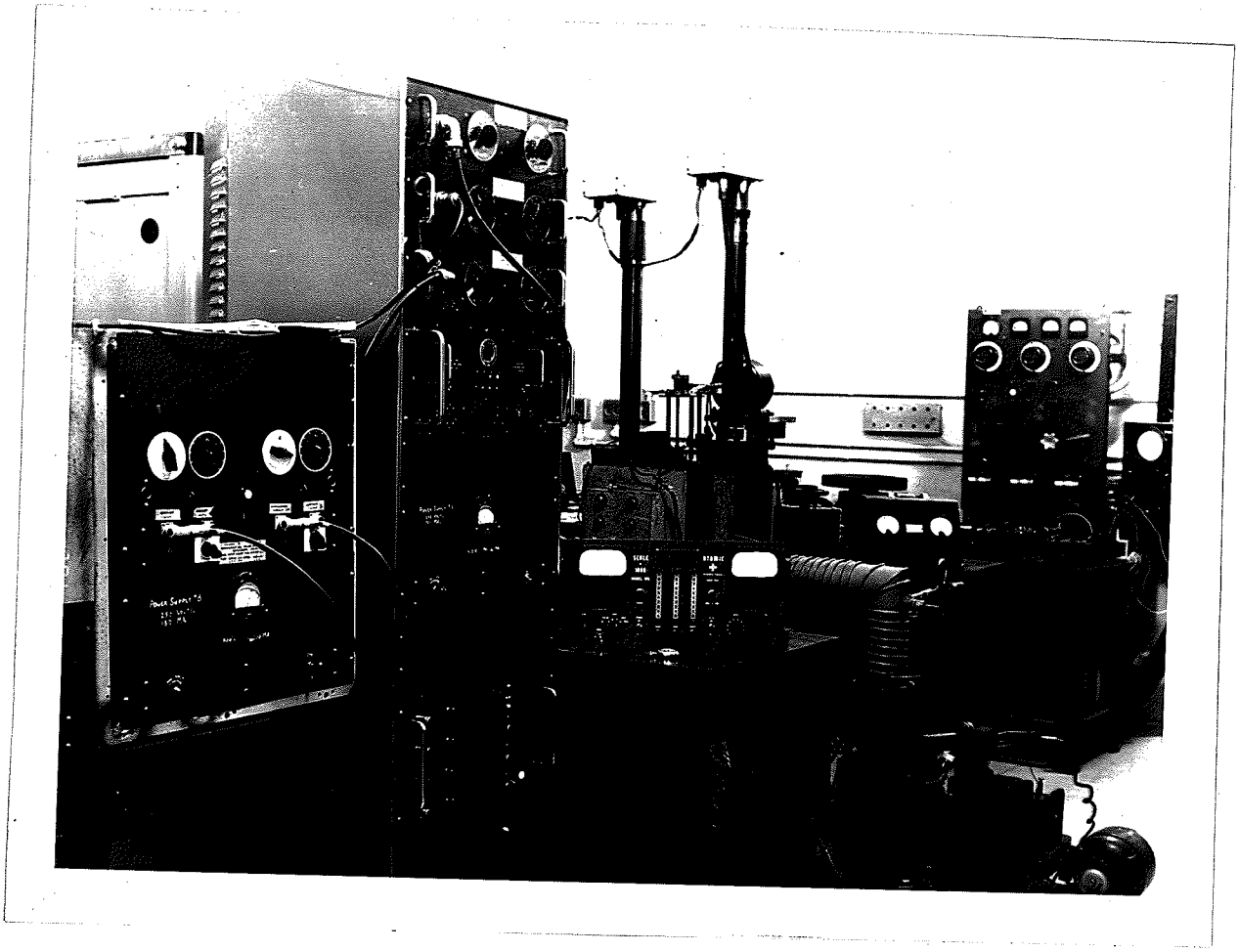

PLATE 8.

View of rack-mounted coincidence equipment.

6. COINCIDENCE INVESTIGATIONS.

6.1 Iridium 192.

Iridium 192 has attracted some attention from nuclear physicists because of the large number of gamma rays associated with its disintegration and its apparently simple beta spectrum. (42-46) The gamma ray energies have been measured with a beta particle spectrometer, using the conversion electrons, and decay schemes have been proposed on the basis of these measurements. As there has been a certain amount of ambiguity about the schemes it was considered that a study of the isotope, using coincidence techniques, might provide sufficient information to enable the ambiguities to be resolved.

The gamma ray scintillation spectrum was, first of all, examined and is shown in Figure 19. A peak is obtained at approximately 312 KeV due, according to beta particle spectrometer measurements, to three gamma rays of energies 295, 308 and 316 KeV. According to Scheef and Hill (46) the relative intensities of these gamma rays are 35, 15 and 100. The scintillation spectrometer has not got a sufficiently high resolution to separate these so that a single peak is obtained. Another peak of considerably less intensity is obtained at 468 KeV and a third at 590 KeV of even smaller intensity. This spectrum was plotted using the 4-channel pulse height analyser, which can analyse pulse heights between 5 volts and 34 volts only. For this reason only a limited energy range can be covered in one run.

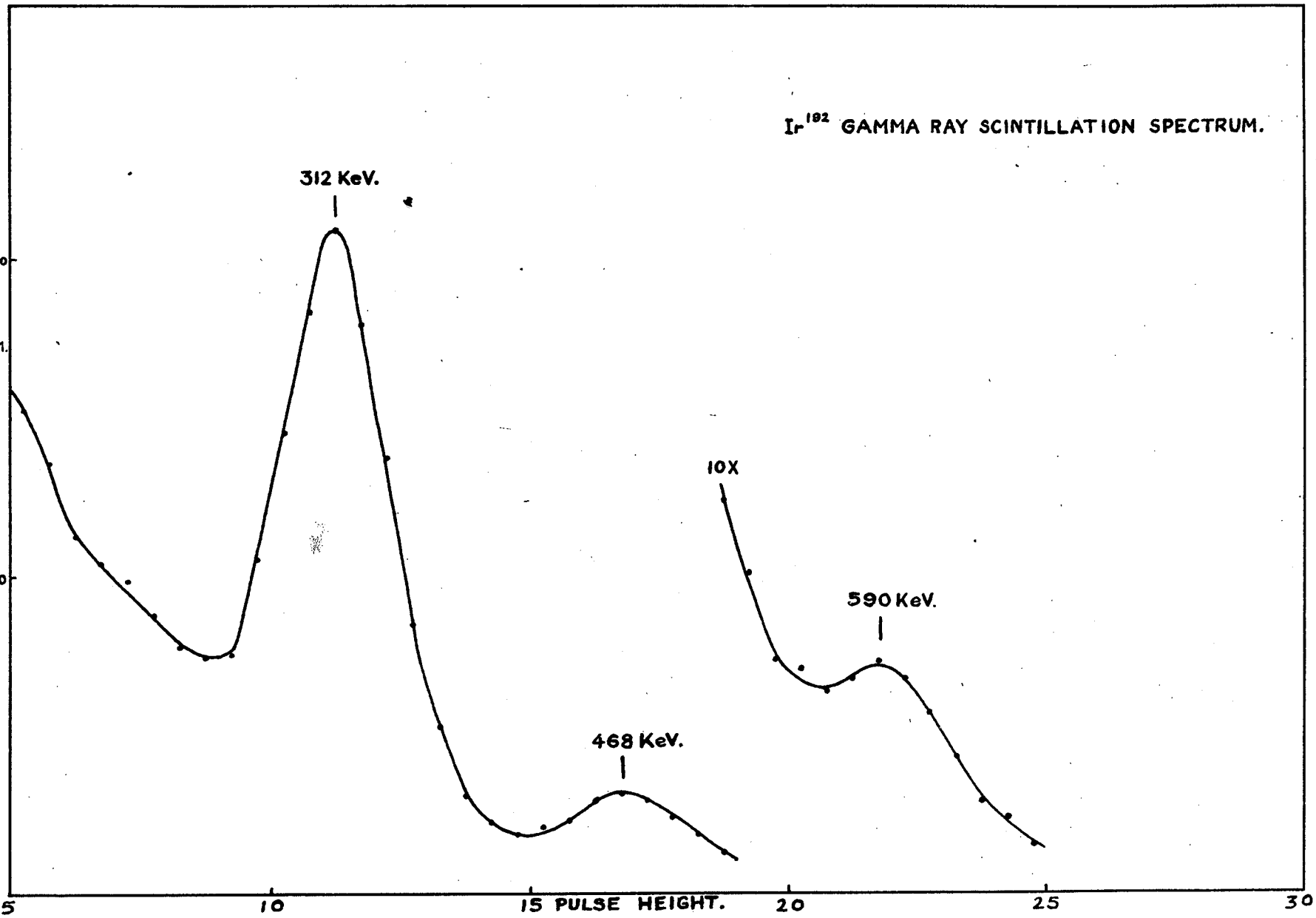
Ir^192 GAMMA RAY SCINTILLATION SPECTRUM.
312 KeV.
2000
C.P.M.
1000
10X
590 KeV.
468 KeV.
5
10
15 PULSE HEIGHT.
20
25
30

FIGURE 19.

The single channel analyser used in the coincidence equipment can be operated over the range 2 volts to 100 volts and can, therefore, cover a much greater energy range. In a plot of the gamma ray spectrum taken during a coincidence run (see Figure 21) other gamma rays and an X-ray are apparent. The X-ray occurs at 64 KeV (the platinum K_{α} line) and gamma rays at 155, 312, 465, 612, 775 and 870 KeV. (These figures are based on a calibration with iodine 131.) The 155 KeV line is probably a combination of lines at 136, 156, and 173 KeV and the 612 KeV line is probably a combination of lines at 589, 604 and 611 KeV. Lines reported at 400, 415 and 439 KeV are of much lower intensity than that at 465 KeV, and probably give a perceptible contribution between the 312 KeV peak and the 465 KeV peak. Two further humps on the distribution curve indicate lines of energies approximately 775 and 870 KeV, but accurate estimation is not possible as clearly defined peaks are not obtained. These lines have not been reported previously in the literature, but Standil has observed that high energy radiation (greater than 611 KeV) does exist (15).

Plate 9 shows an oscillogram of the iridium scintillation spectrum. The broad intense line corresponds to the group at 312 KeV while below it the 155 KeV gamma ray and the X-ray are seen. Above the intense line the 465 and 612 KeV lines can be seen. In Plate 10A a 'Z' modulation type of

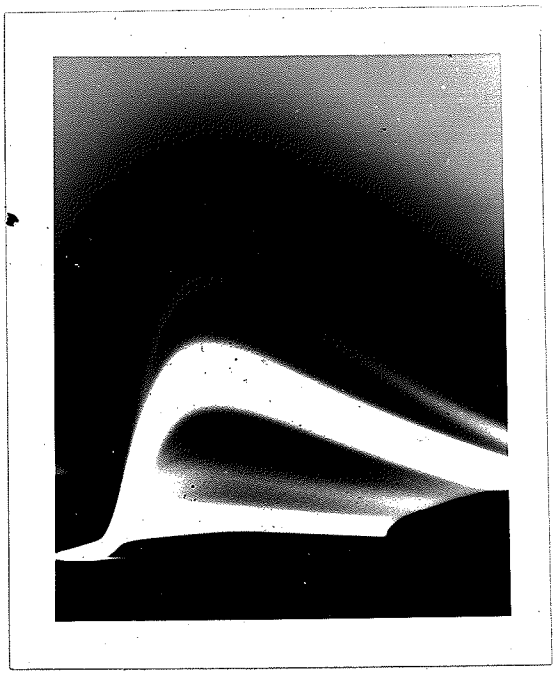

PLATE 9.

Oscillogram of iridium 192 spectrum.

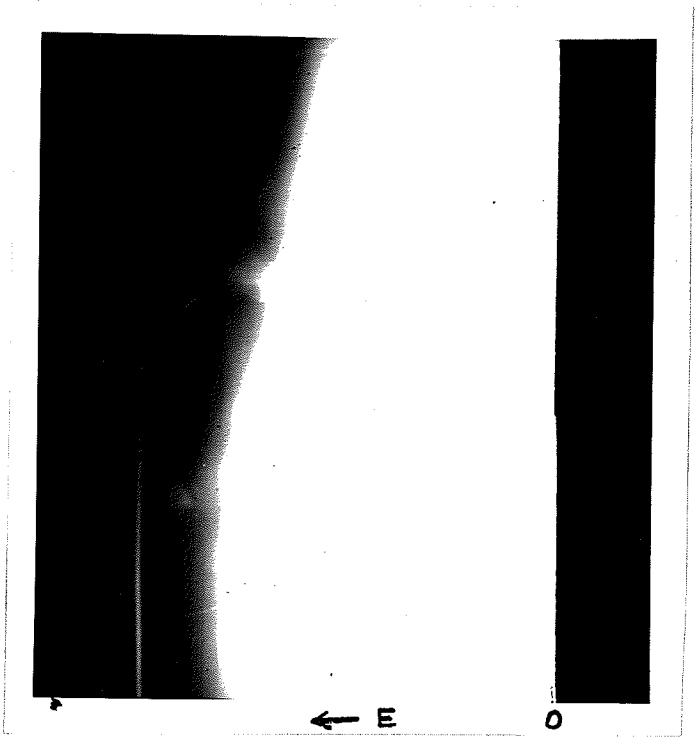

PLATE 10A.

Oscillogram of iridium 192 spectrum.

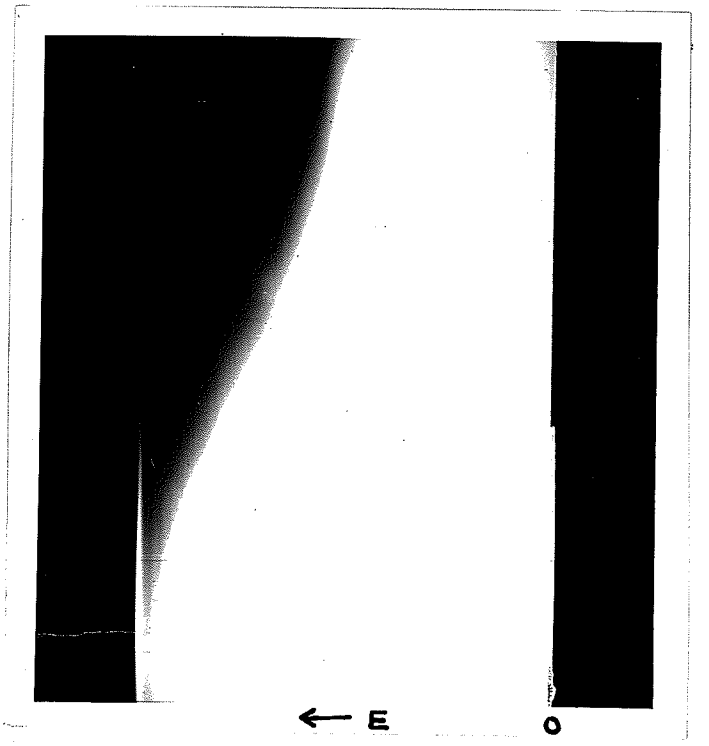

PLATE 10B.

Cobalt 60 calibration oscillogram.

photograph is shown, and Plate 10B is the corresponding photograph for cobalt 60 (for calibration purposes). Examination of Plate 10A shows that there exists high energy radiation as far out as 1.2 MeV and that there are probably several other gamma ray energies in the region 611 KeV to 1.2 MeV. These would not be clearly resolved owing to the superposition of Compton distributions and photoelectron lines, the former becoming more important in this region.

To summarise, gamma rays of energies 775 and 970 KeV have been found in the disintegration of iridium 192 and further gamma rays of energies up to 1.2 MeV exist, although it has not been possible to identify the individual lines.

In the investigation of the decay scheme of iridium 192 it was found desirable to confirm that the total energy involved in the ground-state transition was 1.6 MeV as taken by Cork (45). To do this a small piece of the active source was wrapped in cigarette paper, placed on the side of a sodium iodide crystal and the pulse height distribution curve plotted at the high energy end. For calibration purposes the high energy region of the cobalt 60 gamma ray spectrum was also plotted and the two end-points compared.

The iridium end-point is a combination of the individual beta spectra end-points and the photoelectron lines due to the associated gamma rays, whereas the cobalt 60 end-point is the photoelectron line due to the 1.33 MeV gamma ray.

accurate comparison of the two end-points is clearly not possible but by using several different ways of estimating the end-points a mean figure of 1.56 ± 0.02 MeV was obtained. To make the shapes of the two curves resemble each other as far as possible the position of the cobalt 60 relative to the crystal was chosen to give roughly the same total counting rate as for the iridium 192. The value of 1.56 MeV agrees very well with that of Cork. Figure 20 shows the curves obtained in the total energy determination and the difference in shape between the two curves is apparent.

Figures 21 and 22 show the results of gamma-gamma coincidence experiments, while Figure 23 shows the results of beta-gamma coincidence experiments. In each case a gamma ray energy is selected in channel (2) of the equipment and the gamma ray or beta particle spectrum is scanned in channel (1) at the same time as the coincidence counting rate is determined. In this way errors due to instrument drifts are mainly eliminated. The pulse height band selected in channel (2) for each run is marked at the corresponding place on the spectrum for channel (1).

Analysis of the results showed that the decay scheme as given by Cork (45) was substantially correct as far as it went, but required the addition of several transitions as well as a new energy level. Cork's scheme is based on accurate energy measurements of conversion electrons and the choice of energy

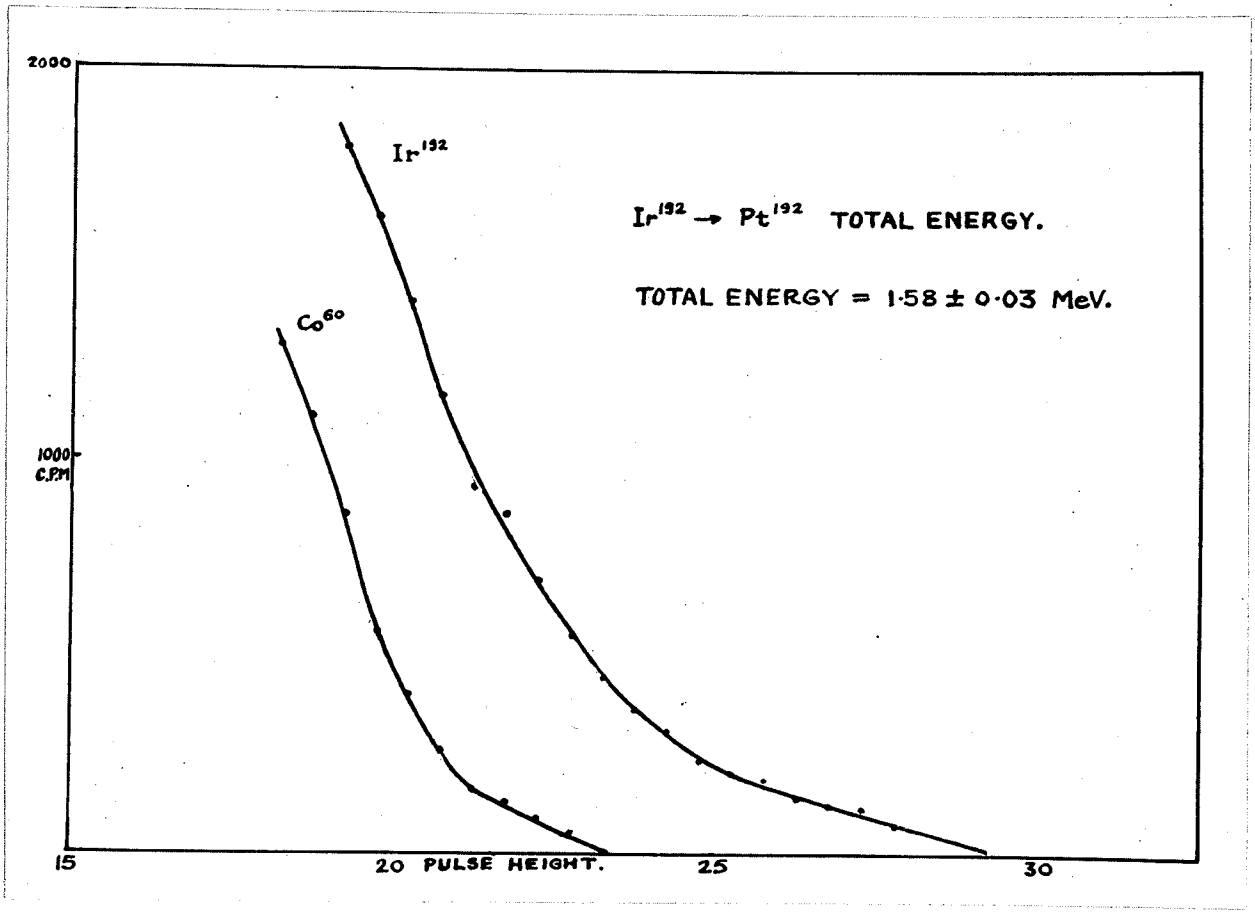

FIGURE 20.

Iridium 192 to platinum 192 total energy.

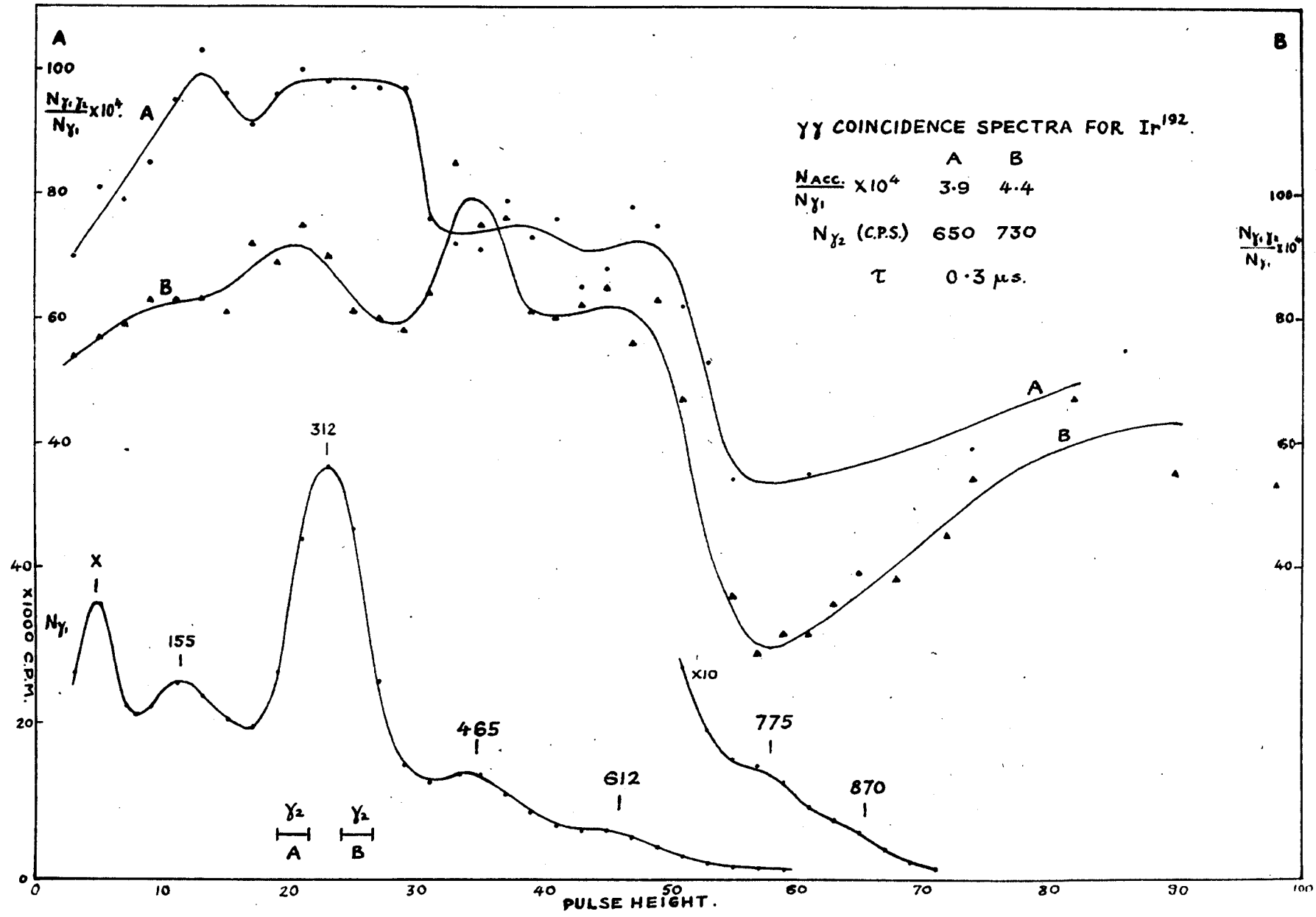
A
B
100
80
60
40
20
0
$\frac{N_{\gamma_1\gamma_2}}{N_{\gamma_1}} \times 10^4$
A
B
γγ COINCIDENCE SPECTRA FOR Ir^{192}.
A B
$\frac{N_{Acc.}}{N_{\gamma_1}} \times 10^4$ 3·9 4·4
N_{γ_2} (C.P.S.) 650 730
τ 0·3 μs.
$\frac{N_{\gamma_1\gamma_2}}{N_{\gamma_1}} \times 10^4$
N_{γ_1} x1000 C.P.M.
X
155
312
465
612
775
870
x10
γ_2 A
γ_2 B
0 10 20 30 40 50 60 70 80 90 100
PULSE HEIGHT.

FIGURE 21.

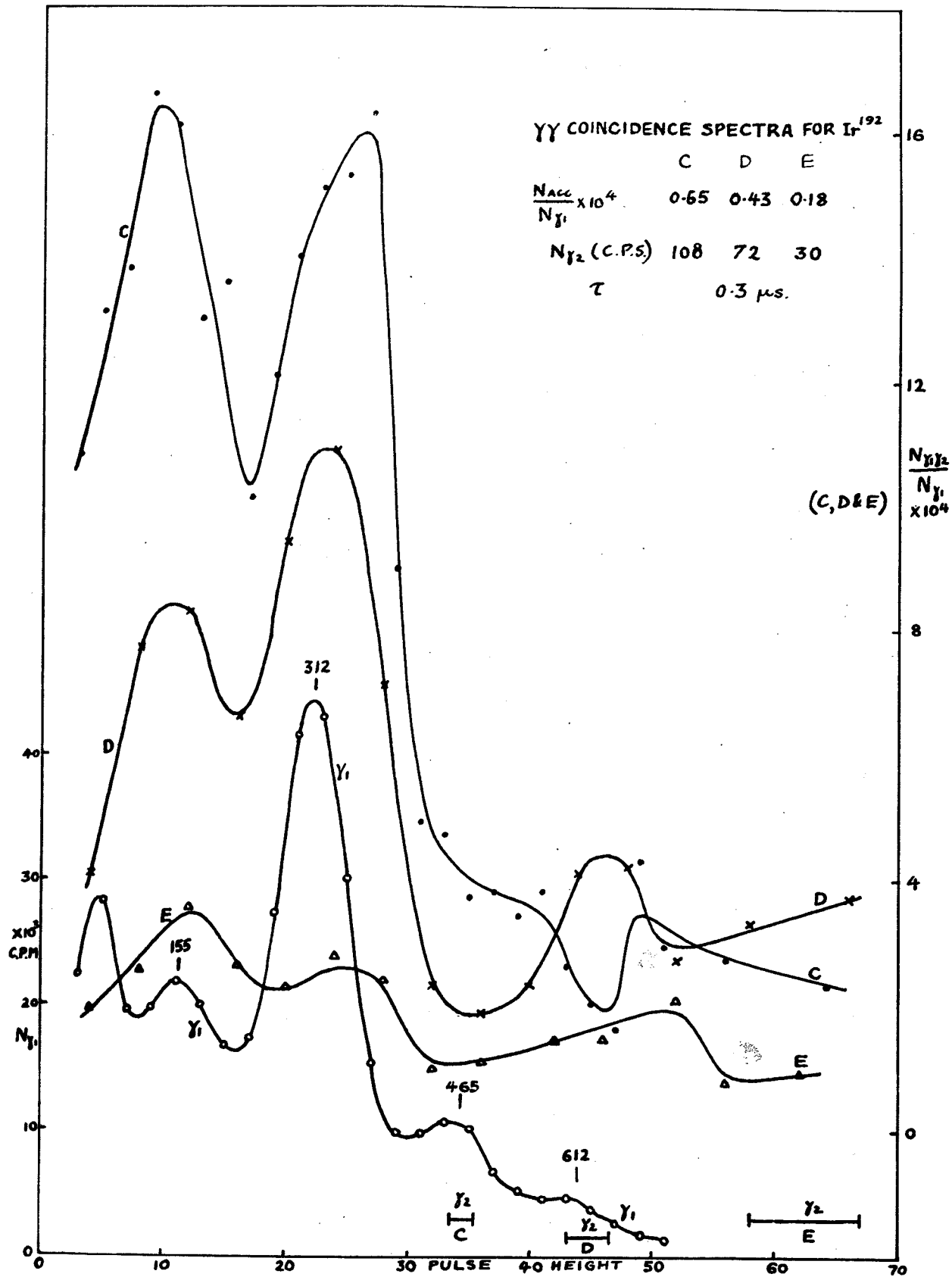
γγ COINCIDENCE SPECTRA FOR Ir192
C D E
Nacc/Nγ1 x10^4 0·65 0·43 0·18
Nγ2 (C.P.S.) 108 72 30
τ 0·3 μs.
Nγ1γ2/Nγ1 x10^4
(C, D & E)
X10^3 C.P.M.
Nγ1
PULSE HEIGHT
312
155
465
612
γ1
γ2
C
D
E

FIGURE 22.

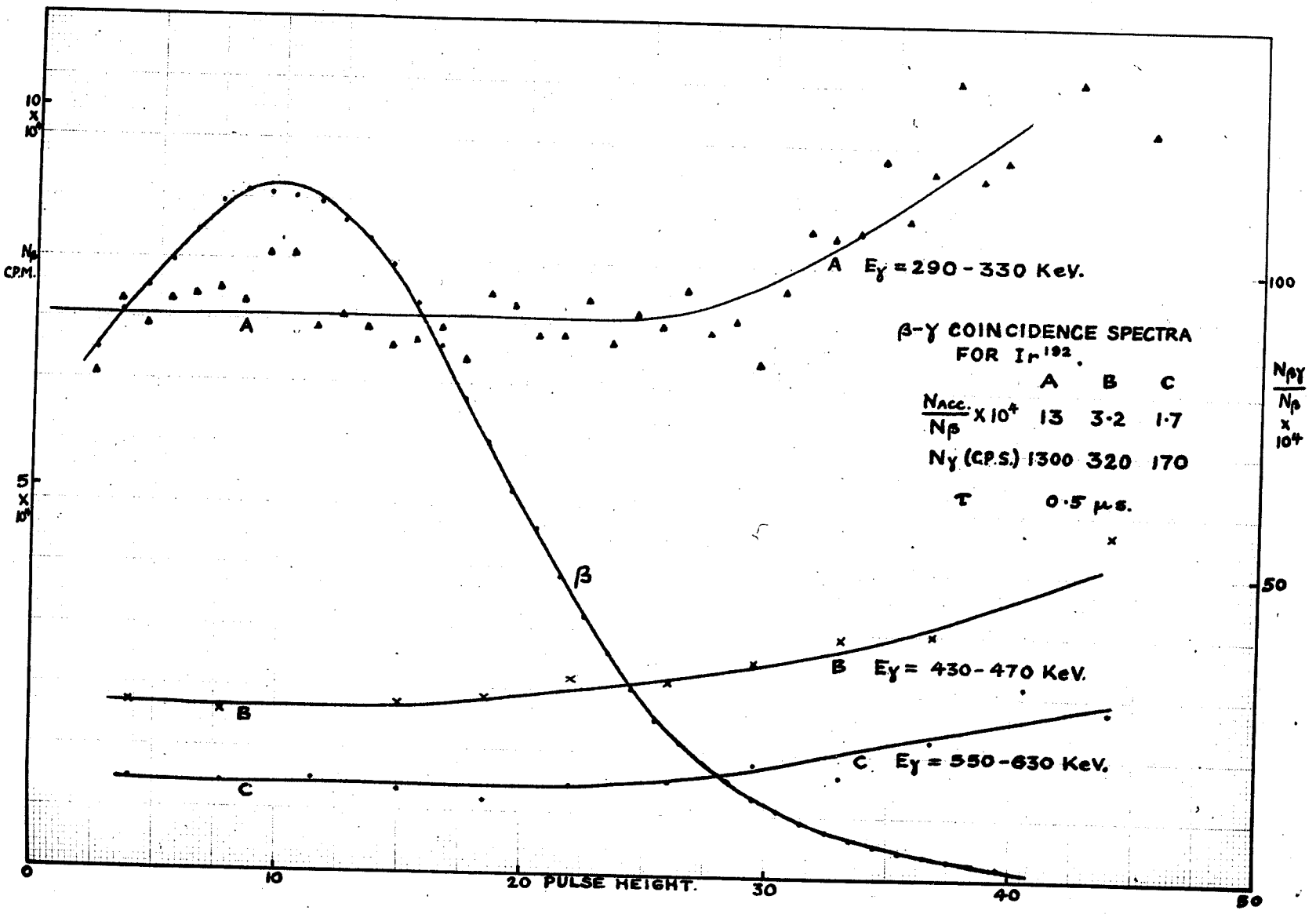
10 x 10³
Nβ C.P.M.
5 x 10³
A
A Eγ = 290 - 330 KeV.
β-γ COINCIDENCE SPECTRA FOR Ir¹⁹²
A B C
Nacc./Nβ X 10⁴ 13 3·2 1·7
Nγ (C.P.S.) 1300 320 170
τ 0·5 μs.
β
B
B Eγ = 430 - 470 KeV.
C
C Eγ = 550 - 630 KeV.
100
50
Nβγ/Nβ x 10⁴
0
10
20 PULSE HEIGHT.
30
40
50

FIGURE 23.

levels to give the appropriate gamma ray energy differences. The proposed decay scheme is shown in Figure 24.

Curve A in Figure 21 is the coincidence curve for pulses arising mainly from the 295 KeV gamma ray. It dips in the region of the X-ray peak. This is to be expected since the X-ray arises from the internal conversion of several gamma rays of different energies and the 295 KeV gamma ray is not likely to be associated with all of these. This same dip is found in all of the coincidence curves and will not be mentioned again. The gamma ray is associated strongly with a line in the 155 KeV group and with the 308 and 316 KeV lines, less strongly with lines in the 465 and 612 KeV regions, less still with 775 KeV but the curve rises beyond this point indicating coupling to higher energy lines. For convenience in referring to the level scheme all the possible transitions have been numbered from 1 to 21. Curve A requires lines 5 and 18 (at least), in addition to those of Cork's scheme. The rise of the curve for energies greater than 775 KeV may be explained by the fact that the pulses occurring in the band A are not all due to the 295 KeV gamma ray, but some fraction must be due to the 308 and 316 KeV gamma rays as well as to higher energy lines.

Curve B shows a strong coupling to the 295 KeV and 465 KeV lines with lesser coupling to the 155 KeV and 612 KeV lines, while the coupling to the 775 KeV region is very small.

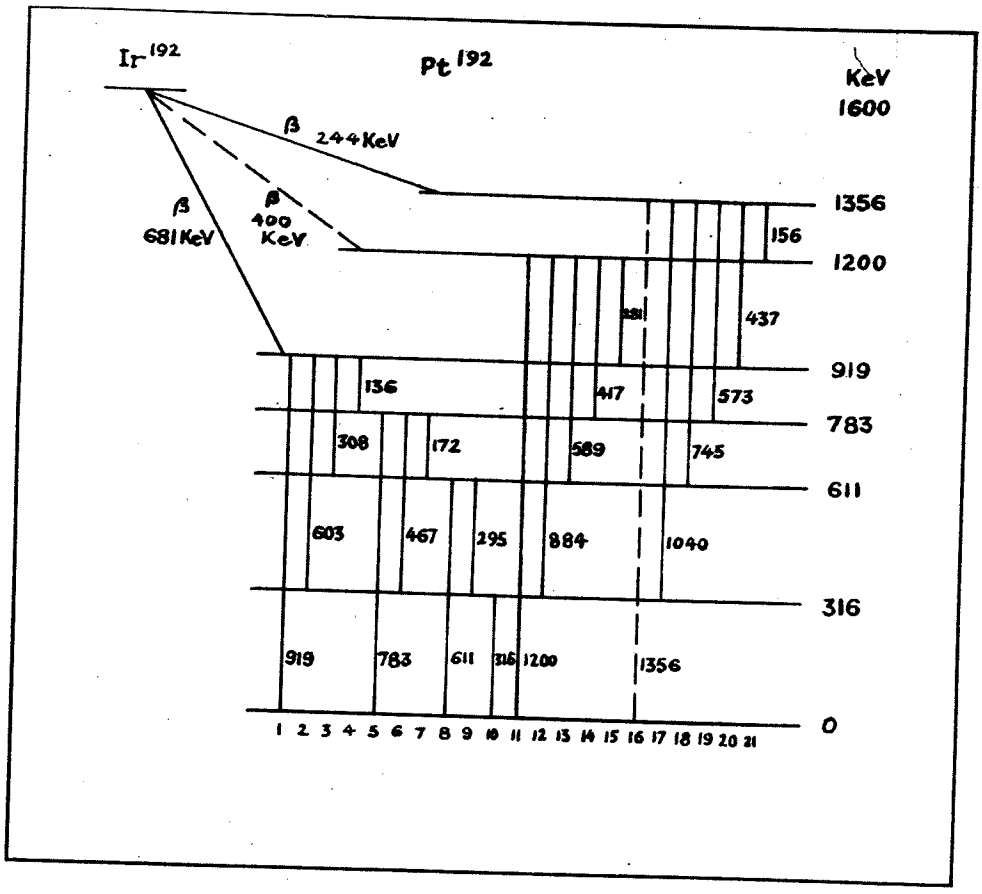

FIGURE 24.

Proposed level scheme for platinum 192 following beta emission from iridium 192.

As with curve A a rise beyond this point is obtained but is more pronounced in curve B. Lines 5, 12, 18 and probably 17 are needed to explain the shape of curve B.

Curve C shows strong coupling to a line about 155 KeV and to the 316 KeV line, but not to the 295 KeV line. There is weak coupling to lines in the 465 KeV region and the region above 612 KeV. At 612 KeV the coupling is very low. The rise above 612 KeV could be explained by the presence of line 14 or line 20 both of which could give rise to pulses in band C and which could be in coincidence with the 611 and 763 KeV lines (8 and 6 respectively in the figure). The presence of line 19 would explain the residual coincidences in the region between 465 and 612 KeV.

Curve D indicates the existence of two lines in the 612 KeV region in cascade, with a higher energy line also in cascade with one or other of them. The addition of line 18 seems to be required for this.

Curve E gives the coincidences with the 800-930 KeV region and requires lines 12 and 21. The existence of the latter line requires an energy level at 1356 KeV. Transitions from this level to the two immediately below it would give lines at 156 and 437 KeV, which Cork et al. have found but have not fitted into their level scheme.

Thus the gamma-gamma coincidence investigations require the addition of lines 5, 12, 18, 21 and possibly 17 to those of Cork's scheme and also the addition of an energy

level at 1556 KeV. The existence of lines 5 and 12 (783 and 884 KeV respectively) seems to be substantiated by the gamma ray scintillation spectrum shown in Figure 21. The oscillogram of the spectrum shown in Plate 10A shows the existence of gamma rays of energy 1.2 MeV. This would justify the inclusion of line 11 in the decay scheme. The fact that no lines seem to be resolved in the region 700 KeV to 1.2 MeV probably indicates the existence of several closely spaced lines. In this region the Compton effect is considerably more important than the photoelectric effect, and this makes it all the more likely that lines will not be resolved. So it is probable that lines corresponding to all the possible transitions actually occur, with that at 1556 KeV very weak.

The beta-gamma coincidence spectra shown in Figure 23 do not add any appreciable information. The coincidence-beta counting rate ratio has a substantially constant value over most of the beta spectrum but rises gradually near the high energy end.

To explain this it must be realised that the beta spectrum obtained from a scintillation spectrometer is very different from that obtained with a magnetic focussing type. In the former both beta particles and conversion electrons emitted at the same instant will generally be captured in the crystal and will give rise to a pulse proportional to the total energy of the two particles. Thus low energy beta

spectra will tend to be pushed out to the higher energy region. There is also the possibility of capture of gamma rays in the crystal which will give much the same effect. These effects could cause the pulses in the higher energy region of the beta spectrum to be due in the main to beta particles belonging to low energy transitions with the result that the coincidence-beta counting rate ratio might increase instead of decreasing, as would normally be expected.

Cork et al. have reported (45) K-L-M differences characteristic of osmium in three of the internal conversion groups they identified in the decay of iridium 192. The gamma rays corresponding to these groups are additional to the transitions indicated in Figure 24. The decay to osmium 192 must have a low probability compared with the beta emission process and has neither been confirmed nor disproved by the experiments described.

6.2. Cerium 141.

Cerium 141 decays to praseodymium 141 by beta emission with a half-life of approximately 30 days (47-49). Beta particle energies of 0.56 MeV (ground-state transition) and 0.41 MeV in the ratio 30:70 have been reported (48) while one group finds a beta particle of 0.25 MeV necessary although this has not been observed (50). Gamma rays are reported at 145 KeV or thereabouts (48, 51, 52) and at 315 KeV (50). The latter gamma ray is considered by Mandeville and Shapiro (53) to be due to an impurity.

Hirzel et al. (54) have reported a meta-stable state in praseodymium 141 at 145 KeV with a half-life of 70 ± 30 microseconds. Ter-Pogossian et al. (50) claim that the 145 KeV gamma ray must be delayed while Mandeville and Shapiro (53) Runyan et al. (55) and Freedman and Engelkemeir (56) do not find a meta-stable state.

In the present investigations the active samples were mounted on very thin aluminum foil for beta spectrometer studies. A dummy foil was also supplied. The first sample received was found to be strongly contaminated with iridium 192 as shown by the gamma ray scintillation spectrum. The second sample was also found to be contaminated with iridium, although much less so. In this case the dummy had roughly twice the contamination activity of the source. However, a small piece of the sample taken from an end, for coincidence

studies, was found to be free of contamination and the results quoted are for this piece.

The gamma ray scintillation spectrum contained a high intensity peak at 145 KeV and an X-ray peak at about 35 KeV. (See Figure 25) In the higher energy region two humps on the curve were observed, at energies of approximately 235 KeV and 370 KeV. Accurate measurements were not possible as the intensities were low compared with that of the 145 KeV line.

Over a short period of time (8 days) it was found that the shape of the scintillation pulse height distribution curve showed signs of having altered. This indicated that the weak high energy lines belonged to a shorter lived isotope but sufficient time was not available to prove this beyond doubt. The half-life of this isotope would be of the order of 20 days.

In investigating the decay scheme it was considered advisable to measure the total energy for the decay, as was done for iridium 192. The same procedure was adopted and cobalt 60 was used for calibration. The end-points of the two curves were compared in several different ways and the mean value of the end-point energies for the cerium was found to be 0.57 $\pm$ 0.02 MeV (see Figure 26). The accepted value of 0.58 MeV has been arrived at by estimation of the end-point energy of a beta spectrum assumed to belong to a ground-state transition. The

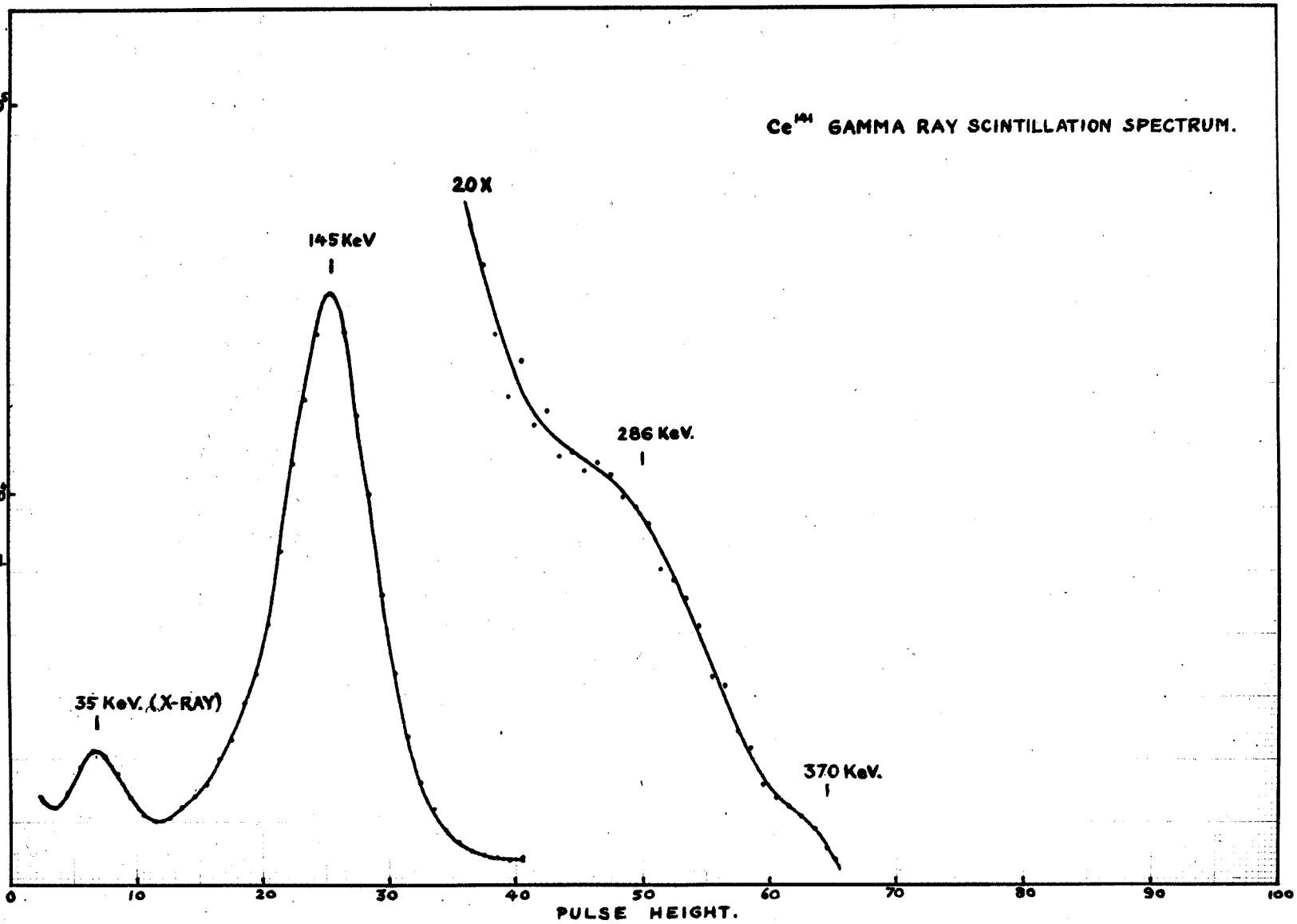
Ce[141] GAMMA RAY SCINTILLATION SPECTRUM.
20X
145 KeV
286 KeV.
35 KeV. (X-RAY)
370 KeV.
C.P.M.
0
10
20
30
40
50
60
70
80
90
100
PULSE HEIGHT.

FIGURE 25.

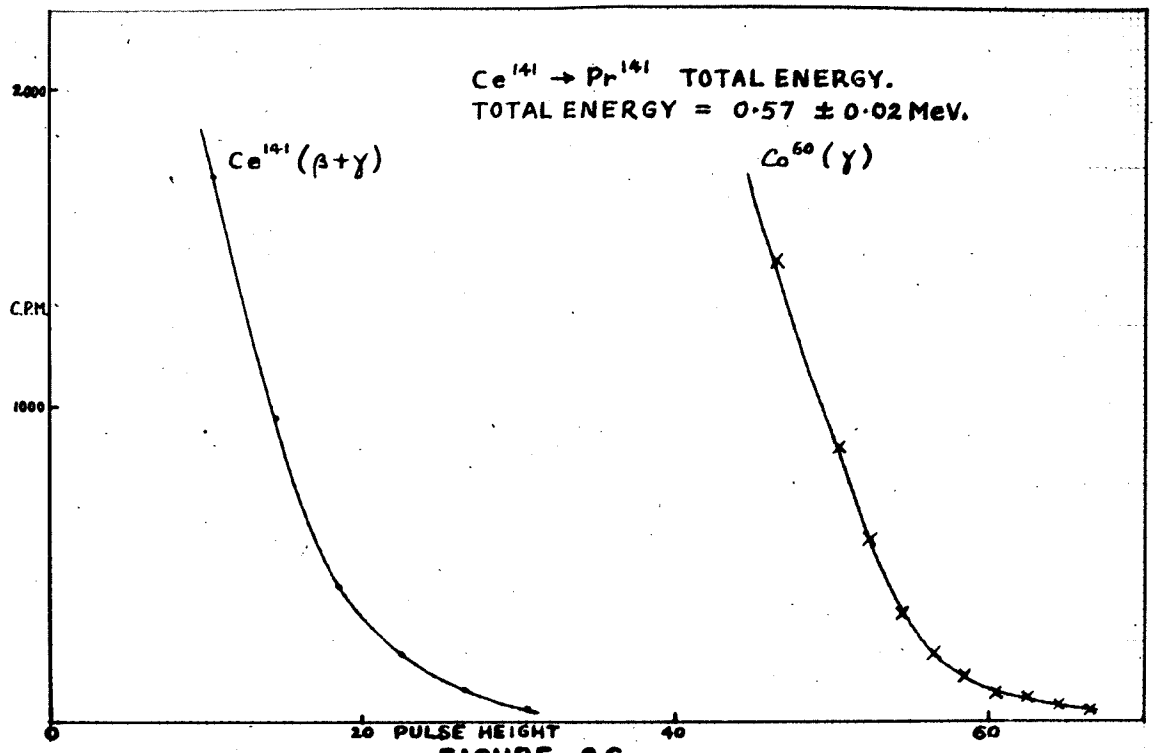

FIGURE 26.

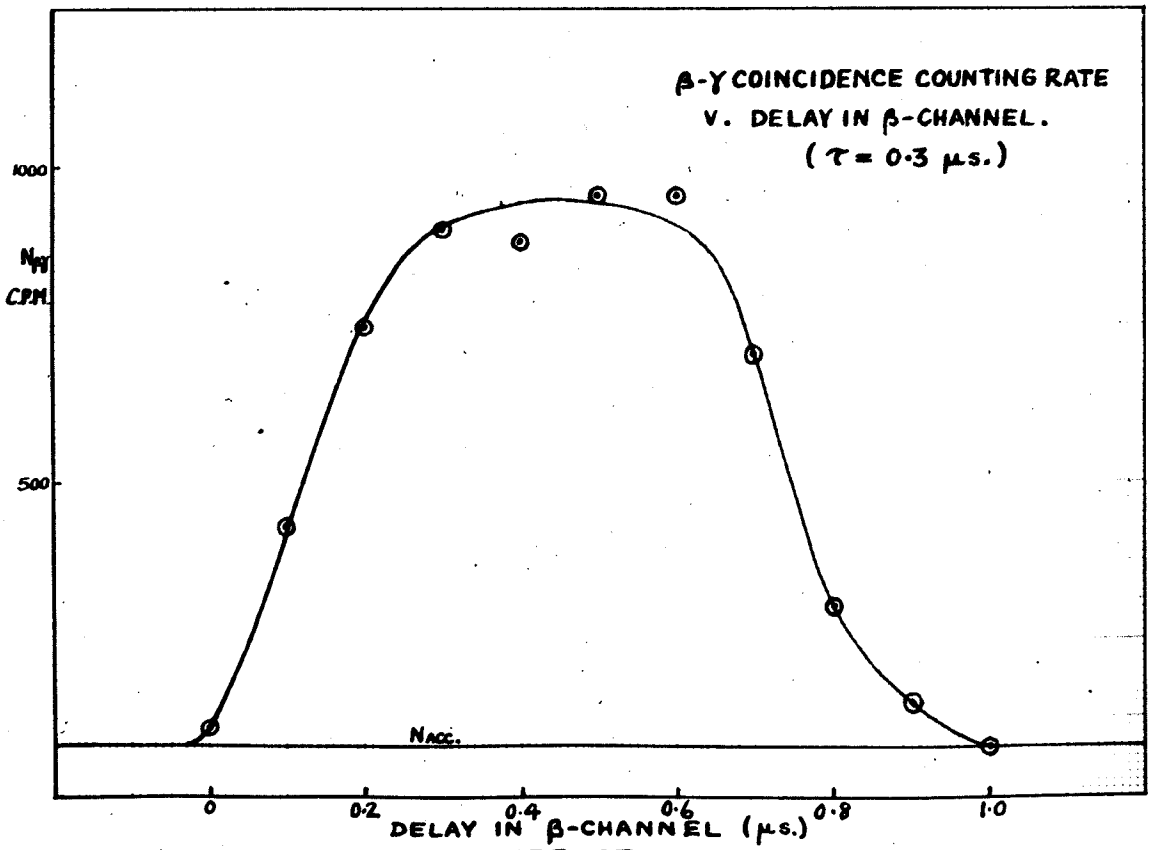

FIGURE 27.

scintillation spectrometer method provides a good check on this figure.

The meta-stable state problem was investigated using the coincidence equipment with the signal-delay facility. Detector heads were set up, one for beta particle detection with an anthracene crystal and the other for gamma ray detection. The 145 KeV peak was selected in the gamma ray channel and a portion of the beta spectrum near the maximum was selected in the beta particle channel. A time delay was introduced in the beta channel starting at zero and increasing in 0.1 microsecond steps to a maximum of 1 microsecond. The coincidence counting rate plotted against time delay is shown in Figure 27. The width of the curve at half-height is 0.62 microsecond and should be 0.60 microsecond for a resolving time of 0.3 microsecond. It will be noticed that the centre of this curve occurs when the delay in the beta channel is 0.45 microseconds. This is due to unequal delays in the two channels and the fact that anthracene gives pulses with a faster rise time than sodium iodide (activated). This is an instrumental effect and in coincidence experiments a delay of 0.4 microseconds was inserted in the beta channel. There is only a slight trace of asymmetry and the tail on the right hand side would suggest an upper limit on the half-life of a possible meta-stable state of less than 0.1 microsecond.

Coincidence experiments were carried out with cerium 141 as was done with iridium 192. The results of the gamma-gamma coincidence investigations are shown in Figure 28. No

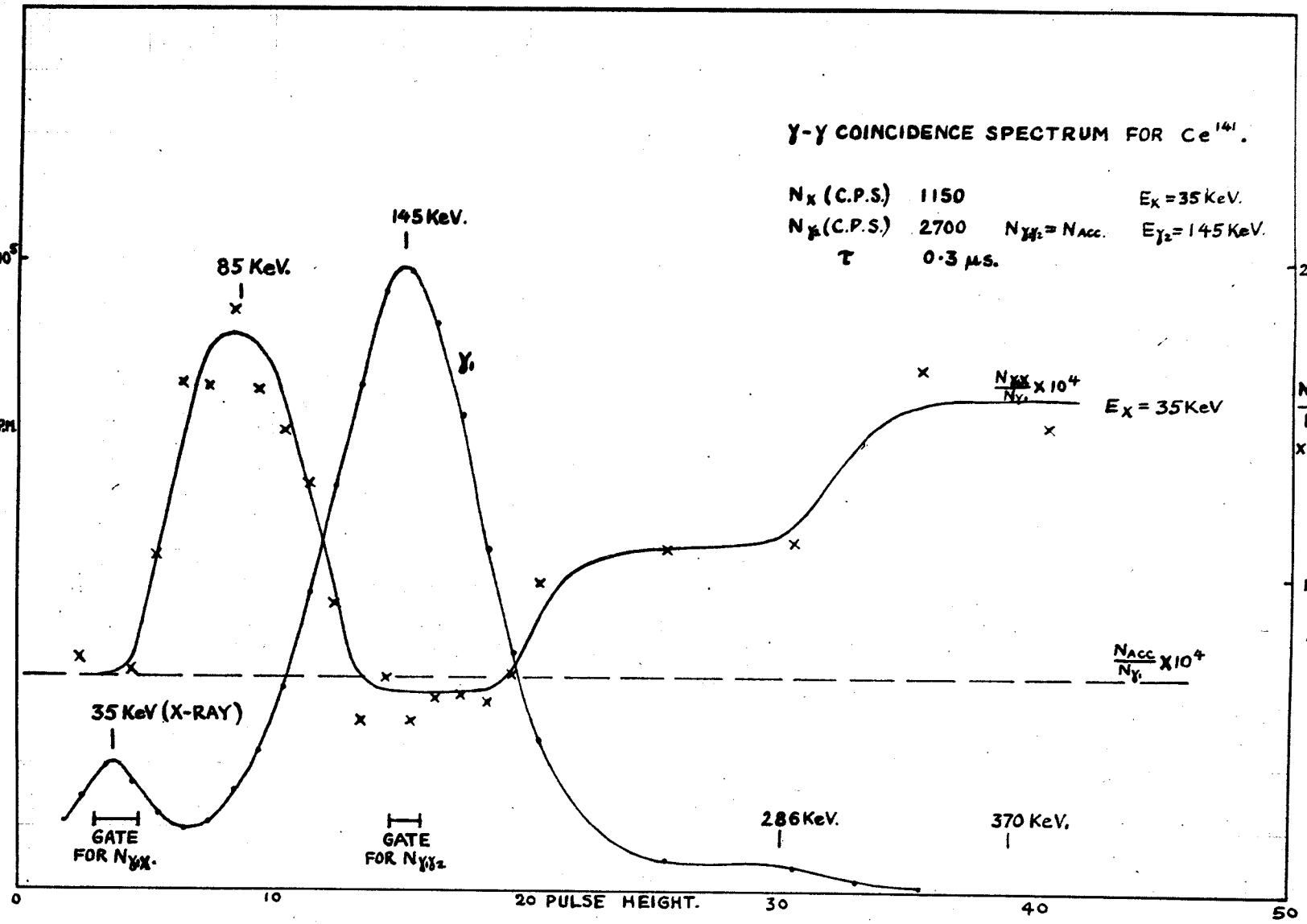
γ-γ COINCIDENCE SPECTRUM FOR Ce 141.
N_X (C.P.S.) 1150
N_γ (C.P.S.) 2700
τ 0·3 μs.
E_K = 35 KeV.
N_γγ2 = N_Acc.
E_γ2 = 145 KeV.
145 KeV.
85 KeV.
γ1
35 KeV (X-RAY)
GATE FOR N_γX.
GATE FOR N_γγ2
286 KeV.
370 KeV.
N_γX / N_γ1 X 10^4
E_X = 35 KeV
N_Acc / N_γ1 X 10^4
N_γγ2 / N_γ X 10^4.
C.P.M.
10^5
20
10
0
10
20 PULSE HEIGHT.
30
40
50

FIGURE 28.

coincidences were found with the 145 KeV gamma ray. On the other hand, certain coincidences were found between the X-ray peak and other parts of the gamma spectrum. At approximately 85 KeV there appeared to be some association and also at approximately 260 KeV and 290 KeV, but at 145 KeV there definitely was no association. Freedman and Engelkemeir (56) have reported finding a line at 216 KeV in the cerium gamma ray spectrum. They attributed this to contamination by thorium which had been activated by the neutron irradiation and had decayed to protactinium 233 which has a half-life of 27.4 days, and emits gamma rays of 84 KeV as well as several in the region of 300 KeV and one at 415 KeV. The results obtained here seem to confirm this view. The gamma rays mentioned can be in cascade with other gamma rays as there are energy levels up to 471 KeV. If and when a gamma ray is internally converted the characteristic X-rays of protactinium will be emitted. The L_{α} X-ray at 16 KeV could give rise to pulses in channel (2) of the coincidence equipment and the associated gamma ray, if detected in the other channel, would give a coincidence count. Moreover, the K_{α} X-ray at 91 KeV might be detected in channel (1) while the associated L_{α} X-ray might be detected in channel (2). Thus the peak at 85 KeV in the coincidence curve could be due to the 84 KeV gamma ray and the 91 KeV X-ray.

The fact that no association is found between the 145 KeV gamma ray and the pulses included in the channel (2)

gate indicates that the 145 KeV gamma ray is not in cascade with others.

Beta-gamma coincidences (see Figure 29) showed the 145 KeV gamma ray to be in coincidence with a beta spectrum of maximum energy about 0.45 MeV. Above 0.45 MeV the $N_{\beta\gamma}/N_{\beta}$ ratio did not drop to the value calculated for accidental counts and this value was maintained up to about 1 MeV. As this is much higher than the total energy involved in the cerium 141 decay, it must be attributed to an impurity. There is the possibility of this impurity being praseodymium 143 which has a half-life of about 14 days. It is formed from cerium 142 which gives cerium 143 under neutron bombardment and which decays to praseodymium 143 with a half-life of 33 hours. It is reported to have a beta particle of maximum energy 0.93 MeV with no gamma rays (57). If the present anomaly is explained in this manner a gamma ray must be associated with the beta particle in this praseodymium 143 decay.

The anthracene crystal spectrometer was calibrated using phosphorus 32 which has a beta particle of energy 1.71 MeV with no gamma rays. (59)

The decay scheme shown in Figure 30 seems to be substantiated by the investigations. There is no evidence supporting a higher energy gamma ray and lower energy beta particle, nor is there any foundation for the existence of a meta-stable state of half-life greater than 10^{-7} second at the 145 KeV level.

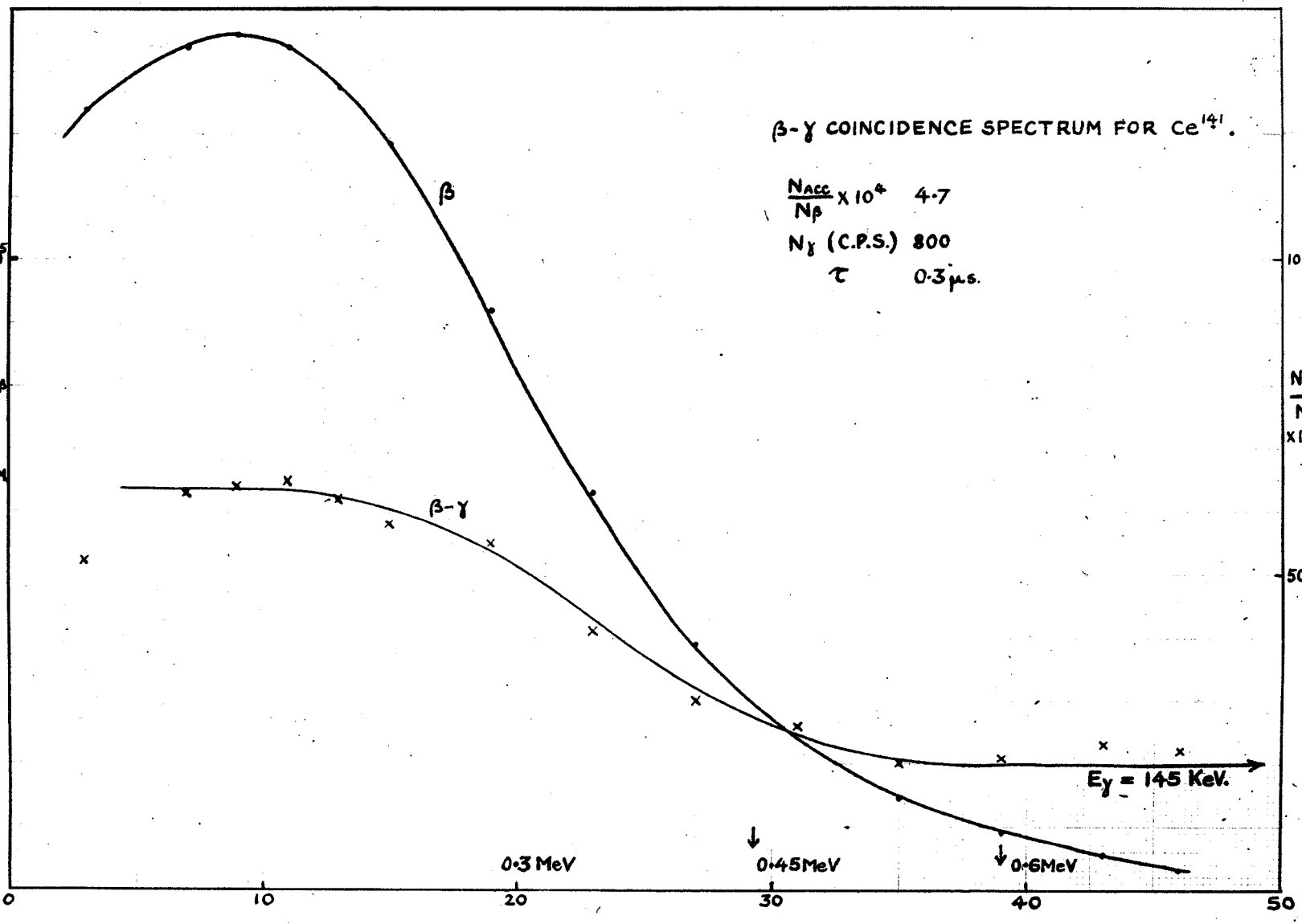
β-γ COINCIDENCE SPECTRUM FOR Ce141.
Nacc/Nβ x 10⁴ 4·7
Nγ (C.P.S.) 800
τ 0·3 μs.
β
β-γ
Eγ = 145 KeV.
0·3 MeV
0·45MeV
0·6MeV
10⁵
Nβ
C.P.M
100
50
Nβγ/Nβ x10⁴
0
10
20
30
40
50

FIGURE 29.

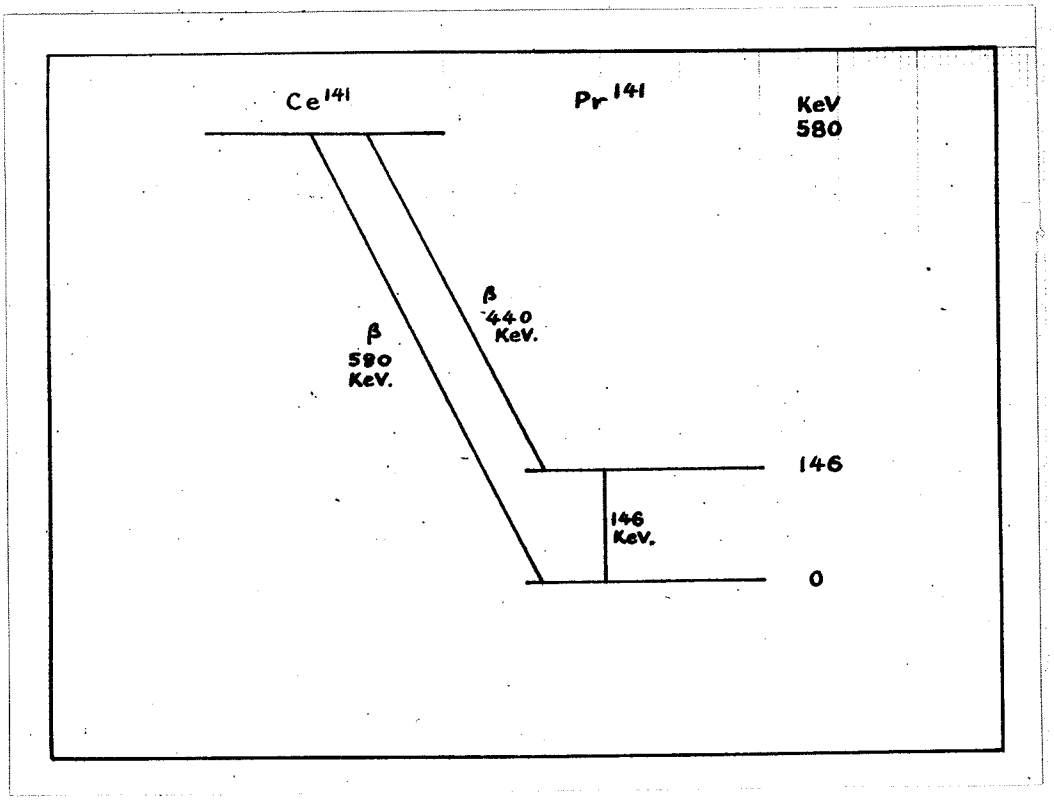

FIGURE 20.

Decay scheme for cerium 141 to praseodymium 141.

7. Conclusion.

The scintillation spectrometer in its present stage of development has proved to be a useful tool in the measurement of gamma ray energies, as proportionality between pulse height and gamma ray energy over a large energy range has been verified. The accuracy and resolution are not as good as those obtained by measurements on conversion electrons with a magnetic beta spectrometer, but it has been possible to measure the energies of gamma rays of intensities much lower than the limit for such spectrometers. The occurrence of the photoelectric and Compton effects and "pair production" have been verified.

In time correlation studies it has been possible to perform experiments in much shorter times than heretofore possible because of the high detection efficiency and the fact that large solid angles may be subtended at the source by the detector. By making use of the scintillation counter as a gamma ray spectrometer it has been possible to determine associations between gamma rays of different energies as well as to study beta-gamma associations. Decay schemes for iridium 192 and cerium 141 have been proposed.

The total energy involved in a ground-state transition has also been measured using a single spectrometer, and a method of measuring the half-life of a meta-stable state in the region of 1 microsecond has been applied to cerium 141.

The theoretical limit of the possibilities of the

spectrometer has not been reached as the energy conversion efficiency (i.e. the energy of photoelectrons emitted at the photocathode divided by the energy of the gamma ray giving rise to them) is still less than 1%. The discovery of more efficient scintillating crystals and radical changes in photocathode design may result in this efficiency being increased perhaps ten-fold. If this is achieved the value of the instrument will have been enhanced very considerably, but a still greater conversion efficiency is required to compete with the beta spectrometer especially for the study of closely spaced lines.

8. REFERENCES.

1. Bleu and Dreyfus — Rev.Sci.Inst., 16, 248 (1945)
2. Klein and Nishina — Z. Physik, 52, 853 (1929)
3. Breuer and Kallmann — Z. Naturforsch., 2a, 439 &642 (1947)
4. Kallmann — Natur u. Technik,(July 1947)
5. Coltman and Marshall — Phys.Rev., 72, 528A (1947)
6. Coltman and Marshall — Nucleonics,1, no.3, 58 (1947)
7. Marshall, Coltman & Bennett — Rev.Sci.Inst., 19, 744 (1948)
8. Coltman — Proc. I.R.E., 37, 671 (1949)
9. Eppstein — J.Sci.Inst., 28, 41 (1951)
10. Houlston — Nucleonics, 7, no.4, 27 (1950)
11. Schmitt — J.Sci.Inst., 15, 24 (1938)
12. Elmore — Nucleonics, 2, no.3, 16 (1948)
13. Puckle — Time Bases (Chapman and Hall, London, 1943)
14. Elmore and Sands — Electronics (McGraw Hill Book Co. Inc., New York, 1949)
15. Standil — Ph.D. thesis (University of Manitoba, 1951)
16. Horton — AECU585 Scintillation Counter Symposium 1949 (USAEC)
17. Pringle — Nature, 166, 11 (1950)
18. Kinsey, Bartholomew and Walker — Phys. Rev., 83, 519 (1951)
19. Schardt and Bernstein — Rev.Sci.Inst., 22, 1020 (1951)
20. Brownell, G.H. — Precambrian, (March 1950)
21. Brownell, G.H. — Economic Geology, 45, 167 (1950)
22. Pringle, Houlston and Brownell,G.H. — Nature, 165, 527 (1950)
23. Deutsch, Elliott and Roberts — Phys. Rev., 69, 193 (1946)

24. Lind, Brown and Du Mond — Phys. Rev., 76, 691 & 1838 (1949)

25. Brownell, G.L. — M.I.T. Progress Report, 1, 57 (Oct.1949)

26. Pringle, Houlston & Taylor — Rev.Sci.Inst., 21, 216 (1950)

27. Metzger and Deutsch — Phys. Rev., 74, 1640 (1948)

28. Pringle and Standil — Phys. Rev., 80, 762 (1950)

29. Ketelle, Boldes, Rossi and Bandl — Phys.Rev., 84, 885 (1951)

30. Pringle, Houlston & Standil — Phys. Rev., 79, 627 (1950)

31. Bradford and Bennett — Phys. Rev., 77, 755 (1950)

32. Ellis — Proc.Roy.Soc.(London), A 143, 350 (1934)

33. Lewis and Bowden — Proc.Roy.Soc.(London), A 145, 235 (1934)

34. Briggs — Proc.Roy.Soc.(London), A 157, 183 (1936)

35. Siegbahn — Arkiv.Mat.Astron. Fysik, 30A, no. 20 (1944)

36. Latyshev — Rev.Mod.Phys., 19, 132 (1947)

37. Cork et al. — Phys.Rev., 82, 681 (1951)

38. Pringle and Isford — Phys.Rev., 83, 467 (1951)

39. Dunworth — Rev.Sci.Inst., 11, 167 (1940)

40. Bothe and von Baeyer — Zeits. f. Physik 95, 417 (1935)

41. Dunworth — Nature, 144, 152 (1939)

42. Levy — Phys.Rev., 72, 352 (1947)

43. Cork — Phys.Rev., 72, 881 (1947)

44. Hill and Meyerhof — Phys.Rev., 73, 812 (1948)

45. Cork et al. — Phys.Rev., 82, 258 (1951)

46. Schoof and Hill — Phys.Rev., 82, 892 (1951)

47. Bothe — Z. Naturforsch, 1, 179 (1946)

48. Shepherd — Research (London), 1, 671 (1948)

49. Burgus and Ballou — NNES9, paper 180. (1950)

50.	Ter-Mogousian et al.	Phys.Rev., 76, 909 (1949)
51.	Hill	Phys.Rev., 82, 449 (1951)
52.	Keller and Cork	Phys.Rev., 83, 216 (1951)
53.	Mandeville and Shapiro	Phys.Rev., 75, 1834 (1949)
54.	Hirzel et al.	Helv.Phys.Acta, 20, 241 (1947)
55.	Runyan, Lundby & Walker	Proc.Phys.Soc.A, 62, 253 (1949)
56.	Freedman and Engelkemeir	Phys.Rev., 75, 897 (1950)
57.	Hallou	NNES, paper 178 (1950)
58.	Siegbahn	Phys.Rev., 70, 127 (1946)